CSIR

Division of Water Technology

Report to the

WATER RESEARCH COMMISSION

on

PILOT STUDIES ON PHOSPHATE CRYSTALLIZATION IN BIOLOGICAL WASTEWATER TREATMENT SYSTEMS

by

P A Loots

R A Oellermann

K Pearce

G B Saayman

WRC Report No. 366 /1/94
ISBN 1 86845 128 3

PRETORIA
November 1994

PILOT STUDIES ON PHOSPHATE CRYSTALLIZATION IN BIOLOGICAL WASTEWATER TREATMENT SYSTEMS

by

G B Saayman

City Council of Pretoria
P O Box 1409, Pretoria 0001, South Africa

and

P A Loots, R A Oellermann and K Pearce

Water, Waste & Effluent Treatment
Division of Water Technology, CSIR
P O Box 395, Pretoria 0001, South Africa

Final Report to the Water Research Commission on the Project
"Pilot Plant Studies on Full-Scale Phosphate Crystallization in Biological Systems"

WRC Project No: K5/366
CSIR Project No: WD004 6800 6840

Programme Manager: Mr A Gerber
Project Leader: Dr R A Oellermann

October 1994

EXECUTIVE SUMMARY

MOTIVATION AND BACKGROUND

Phosphate has been identified as a major nutrient in the problem of eutrophication of water. During the past decades a number of promising technologies have been researched to achieve efficient and effective phosphate removal from effluent. Among these was the introduction of crystallization which potentially represents a clean, cost effective and efficient approach to alleviating this pollution problem.

PROJECT AIMS

A pilot-scale evaluation of a fluidized sand bed reactor was to be conducted on a phosphate-rich effluent abstracted after anaerobic treatment. A suitable reactor configuration was to be established and the critical design and operational aspects on which the successful commissioning and maintenance of the crystallizer will depend, be determined. The integrated system was not to exceed the effluent standard of 1 mg/ℓ (as P) in the combined effluent. Guidelines on the integration of the crystallization technology into a full-scale treatment works were to be compiled and the economics of the process established.

ACHIEVEMENT OF OBJECTIVES

Phosphate crystallization is a relatively recent technological development and a number of unforeseen obstacles were experienced in the design and operation of the pilot plant. The original objectives set for the investigation were therefore modified during the course of the investigation by the Steering Committee. It was decided to concentrate the research efforts on the pilot-scale crystallization and no full-scale evaluation was conducted. The effect of integration of the crystallizer into an activated sludge system was therefore also neglected. It was considered that this objective was of lesser importance and the probability of having a major influence on the performance of the activated sludge system would be small.

The emphasis in this investigation was on the pilot-scale evaluation. However, chemical modelling and laboratory investigations were resorted to in order to be more effective in the studies at pilot-scale. The limitations of the laboratory system at low flow rates resulted in the accrual of limited data on some objectives, particularly those subsidiary to correct design and proper operation. However, the data and knowledge gained in solving the problems fundamental to process performance was adequate to provide a crystallizer design and consider operational aspects for the successful implementation of the crystallizer technology, integrated with municipal treatment works. Since the crystallization technology is relatively new and not established in South Africa, the economic evaluation of the system was discussed (see section 5-5). It would be of value of value to evaluate and collate performance data at pilot and full scale to improve the crystallizer design.

CHEMICAL MODELLING

The objective of this component of the study was to apply a dynamic chemical model, viz. the Joint Expert Speciation System (JESS), to the problem of removal of phosphates by precipitation with calcium. It has been suggested, on empirical evidence, that the presence of carbonate at elevated concentration (5 mM) leads to inefficient crystallization of phosphates, and concomitant crystallization of calcium carbonate.

The simulations suggest that the crystallization process is governed by the relative rates of precipitation of the solids present. The most stable phosphate-containing solid possible in the system, hydroxyapatite (HAP) forms slowly, and less stable solids, octacalcium phosphate (OCP) and tricalcium phosphate (TCP) either also form simultaneously, or form instead of any HAP. Under these conditions, if calcium is scavenged by precipitation of calcium carbonate, removal of phosphate is predicted to be low.

Therefore, to optimize phosphate removal, it is desirable to remove carbonate. The method suggested is a lowering of the pH by addition of sulphuric acid, removal of the carbonate as carbon dioxide by venting, and re-adjustment of the pH with lime slurry. This process was simulated by JESS, and it was found that the sulphate added as sulphuric acid to effect the pH reduction was low enough in concentration so as not to interfere with subsequent crystallization of calcium phosphate species. The model also showed that the proposed method of carbonate removal was a viable process.

LABORATORY EVALUATION

The recycle ratio is an important variable to consider for establishing crystallization efficiency. At constant flow, an increase in the recycle ratio results in an increase in the hydraulic retention time. The influent o-phosphate concentration is reduced, with a resultant positive influence on the crystallization effectivity. At low recycle ratios floc carry-over increases, whereas, at high recycle ratios $CaCO_3$ precipitation will occur preferentially, thus increasing the concentration of o-phosphate in the outflow.

Effective venting of the influent at low pH reduces the concentration of the interfering carbonate, hence phosphate is preferentially removed from the effluent at all pH values.

As expected, after carbonate removal the concentration of o-phosphate in the outflow continued to decrease with increasing pH. This effect is not as noticeable at high recycle ratios where the reactor configuration is closer to a completely mixed, rather than a plug flow system. Degassing should therefore have a favourable effect when all other critical performance requirements have been met.

PILOT-SCALE STUDIES

It was difficult to control and maintain optimum process conditions in the pilot plant and the variability of the results did not permit any conclusions on steady-state conditions. However, the results enabled a comparison of the different combinations of interacting parameters

important to effective crystallization.

Fluctuations in the o-phosphate concentration of the feed to the pilot plant had a significant effect on the crystallization performance.

Stringent pH control is the most important operational parameter and is critical for efficient crystallization and reliable performance.

Degassing seems to increase the rate of o-phosphate crystallization but also increases the 'carry-over' of o-phosphate flocs.

Under the prevailing conditions, considerable 'carry-over' of o-phosphate flocs was observed and sufficient crystallization could not be achieved. Recycling is needed to stabilize the process, but the return of flocs should be kept at a minimum to reduce any adverse effect on the crystallization performance. This indicates the requirement of filtration of the flocs from the effluent discharge before recycling, to effect optimum crystallization and to ensure an effluent with a low o-phosphate concentration.

ECONOMICS OF CRYSTALLIZATION

The maintenance of carbonate levels below 2 mM, to ensure effective phosphate removal, effects the economics of the crystallization technology. When degassing is required, the treatment costs, based on the use of sodium hydroxide, amounts to approximately R2,11/m^3. This can be reduced to approximately R1,02/m^3 if degassing is not essential. The cost of chemicals for degassing thus contributes substantially to the treatment costs. However, only a portion of the total anaerobic effluent flow needs to be treated to reduce the phosphate load on the biological phosphate removal system. Thus, if only 10% of the total effluent flow needs to be treated in a crystallizer the foregoing costs, expressed in terms of total effluent flow, reduces to 21 cents/m^3 and 10 cents/m^3, respectively.

At the prevailing rates, the cost of using lime is only 27% of that of sodium hydroxide. However, the lower solubility of calcium hydroxide would require an additional mixing tank, which partially offsets the savings by using lime. When calcium hydroxide is used instead of sodium hydroxide the direct operating cost is reduced by 26%.

TECHNOLOGY IMPLEMENTATION

The feasibility of phosphate crystallization has been demonstrated and the major design criteria determined. To implement the technology successfully, requires the following:

- Proper crystallizer design, specifically the inlet system is extremely important and is considered in detail in the report.

- Suitable quartz sand should be used as crystallization seed material in the fluidized bed.

- The first step in commissioning should be to establish or maintain a stable and adequately fluidized bed at a linear upflow velocity between 40 m/h to 80 m/h.

- A recycle ratio of less than 7 should be used for effective performance of a full-scale crystallizer with a minimum of 1, dependent on the economics of the treatment.

- The mass ratio of Ca:P in the crystallizer influent should be as close as possible to the 2:1 stoichiometric requirement.

- Effective CO_2 degassing of water with a high alkalinity is required to reduce the total carbonate content below 2 mM, in order to produce crystals resistant to abrasion and to minimize 'carry-over' of o-phosphate flocs.

- Concentrated sulphuric acid (98%) can be used for achieving the required degassing pH of 4,8 to 5,0 and 1% sodium hydroxide or 2% milk of lime to maintain the crystallization pH between 9,8 to 10,5. Lime [$Ca(OH)_2$] can be used where calcium supplementation is required, even though its lower solubility implies additional mixing equipment.

- A suitable automated control system for stringent crystallization pH control is an absolute necessity for effective process performance. In this regard special attention must be given to the inhibiting effect of crystallization on an in situ pH measuring electrode.

- A slow steady start-up period of 3 to 4 weeks is recommended to establish stable operational conditions for a full-scale crystallizer (Eggers *et al.*, 1991a,b).

- Filtration of 'carry-over' flocs from the crystallizer effluent is necessary to obtain a very low o-phosphate concentration (< 1 mg P/ℓ), particularly when recycling of the effluent to the crystallizer inlet is applied.

- The economics of the technology needs careful consideration and is determined by the specific application needs.

FUTURE RESEARCH

Laboratory investigations have shown that an increase in the recycle ratio from minimum fluidization to approximately 7 resulted in improved crystallization effectivity. Data on crystallization of phosphate at low recycle ratios was scant. However, DHV in The Netherlands used a recycle ratio of approximately 1. Further work should therefore be done to establish the optimum recycle ratio.

At higher recycle ratios, influent and the recycle stream mixing could result in phosphate precipitation before the sand bed above certain pH levels. Further investigation will be required to prevent such precipitation and optimise the crystallization efficiency.

Carbonate levels above 2 mM interfere with the crystallization process. Further testing should therefore be carried out on degassing under steady state conditions.

It was not possible to investigate the cost-effectivity of filtration to remove flocs making it imperative that this aspect be further investigated. The need of filtration was indicated by the fact that DHV in The Netherlands, who have implemented the crystallization technology at full scale in Europe, made use of filtration in their full-scale applications.

A full-scale evaluation was not been possible in this investigation. To improve on the design specifications, therefore, full-scale studies of phosphate crystallization should be conducted to contribute to the establishment of the technology in South Africa.

Finally, a benefit of crystallization is the recovery of phosphate. The best method of abstraction of large pellets and the frequency of such abstraction during operation should be clarified.

ACKNOWLEDGEMENTS

The research reported on was funded by the Water Research Commission under project K5/366 and entitled "Pilot Plant Studies on Full-Scale Phosphate Crystallization in Biological Systems".

For the duration of this project, the following persons served on the Steering Committee and their valuable contributions are gratefully acknowledged:

Dr T C Erasmus	Water Research Commission (Chairman).
Mr D Huyser	Water Research Commission (Secretary).
Ms A M du Toit	Water Research Commission (Secretary).
Dr S A Mitchell	Water Research Commission.
Mr F J de Wet	City Council of Pretoria.
Mr G B Saayman	City Council of Pretoria.
Mr A Gerber	Division of Water Technology, CSIR.
Ms G A Momberg	Division of Water Technology, CSIR.
Ms K Pearce	Division of Water Technology, CSIR.
Mr P A Loots	Division of Water Technology, CSIR.
Dr R A Oellermann	Division of Water Technology, CSIR.

We are grateful for the constructive inputs and continued interest of Mr A Gerber, Programme Manager of Water, Waste and Effluent Treatment, Division of Water Technology, CSIR, Pretoria and the valuable support of Mr J Scheepers of the Division of Water Technology, CSIR, Daspoort.

We thank Mr D R Wilson of the City Council of Pretoria for the first design of the crystallization column and settler.

The significant contributions by Dr K Murray, Dr P Wade and Ms R Jooste of the Water Quality Information Systems programme of the Division of Water Technology, CSIR on the chemical modelling and chemistry of the crystallization system are gratefully acknowledged.

A special word of thanks to all our colleagues who contributed to the successful completion of this project.

CONTENTS

LIST OF TABLES

LIST OF FIGURES

LIST OF SYMBOLS AND ABBREVIATIONS

Symbol/Abbreviation

A	=	Area (m^2)
ACP	=	Amorphous calcium phosphate
Cd	=	Orifice coefficient
CSIR	=	Council for Scientific and Industrial Research
CSTR	=	Continuously stirred tank reactor
CT	=	Total carbonate
D	=	Diameter (column) (m)
Dp	=	Diameter (particle) (mm)???
d	=	Diameter (particle/nozzle) (mm)
DCPA	=	Monetite
DCPD	=	Brushite; Calcium phosphate dihydrate
Eff(A)	=	Effluent - acidified
Eff(F)	=	Effluent - filtered
FAP	=	Fluoroapatite
HAP	=	Hydroxyapatite
HRT	=	Residence time (h)
HTMP	=	Hydrated trimagnesium phosphate
IAP	=	Ionic activity product
ID	=	Internal diameter
JESS	=	Joint Expert Speciation System
L	=	Length (bed height) (m)
Lo	=	Resting bed height (m)
ℓ	=	Litre
M	=	Molar
mM	=	Millimolar
Mℓ	=	Megalitre
MAP	=	Magnesium hydroxyapatite
MCP	=	Monocalcium phosphate
MFAP	=	Magnesium fluoroapatite
N	=	Specific number ($1/m^2$)
n	=	Number
OCP	=	Octacalcium phosphate
Pa	=	Pascal
Pe	=	Peclet number
PLC	=	Programmable logic controller
PMP	=	Potassium magnesium phosphate
Q	=	Volumetric flow rate (m^3/h)
R	=	Recycle ratio
Re	=	Reynolds number
RTD	=	Residence-time distribution
S	=	Specific surface area (m^2/kg)
SI	=	Saturation index
TCP	=	Whitlockite; Tricalcium phosphate
TMP	=	Trimagnesium Phosphate
Um	=	Linear fluid velocity
u	=	Linear velocity (m/s)
V	=	Volume (m^3)

Symbol

ΔG	=	Energy change
ΔH	=	Enthalpy change
ΔP	=	Pressure change
ΔS	=	Entropy change
ϵ	=	Voidage
μ	=	Viscosity ($N.s/m^2$)
ρ	=	Density (kg/m^3; g/cm^3)
σ	=	Relative supersaturation
ϕ	=	Size distribution factor
ψ	=	Sphericity

Subscript

b	=	Bed
d	=	Distributor
e	=	Effluent
f	=	Feed
m	=	Medium (liquid effluent)
noz	=	Nozzle
or	=	Orifice
p	=	Particle
r	=	Recycle
s	=	Solid
sp	=	Solubility product
t	=	Influent

I. INTRODUCTION

1.1 INTRODUCTION TO PHOSPHATE REMOVAL

Phosphate is one of the key nutrients causing eutrophication of water systems. Therefore, to protect the environment and minimize pollution, the levels of phosphate must be reduced in the discharge by appropriate treatment of effluent. In terms of the South African Water Act (1956), as amended, the special phosphate standard for effluent discharge is 1 mg P/ℓ. The treatment of eutrophic water to potable quality is more complex than that of non-eutrophic water and the economy demands that cost-effective solutions be found to solve the problem.

Phosphorus removal methods include chemical precipitation and biological processes. In wastewater with relatively low concentrations of phosphate, an iron contactor has been shown to be successful (Momberg & Oellermann, 1993). Crystallization technology is a relatively recent introduction of a clean technology since little or no sludge is produced and a product of value can be recovered. It has been evaluated on laboratory scale (Momberg, 1993b).

This report presents the results of a pilot scale evaluation of the crystallization of phosphate at elevated pH in a fluidized sand bed.

To illustrate the complexity and provide an understanding of the crystallization of phosphate in wastewater systems, some background information on the thermodynamics and kinetics of the chemistry of such systems and the actual crystallization process is provided. During the course of the research, laboratory evaluations were undertaken to expedite the pilot evaluations. In this work chemical modelling was an additional tool used to predict the outcome of experimentation, thereby, resulting in more effective research.

1.2 MOTIVATION AND BACKGROUND

The Department of Water Affairs (1986) had identified four main problems related to water quality in South Africa, viz.:

- Salination associated with the increasing intensity of use and reuse of water resources.
- Eutrophication associated with urbanization, urban wastewaters and nutrient-rich effluents and some agricultural practices.
- Trace metals introduced into the water environment by chemical and industrial waste, mining activities, sewage sludges, urban runoff and atmospheric deposition.

- Micropollutants, essentially synthetic chemicals, resistant to physical, chemical or biological degradation, accumulating in aquatic organisms and hence in the food chain, and their concomitant toxic, carcinogenic or teratogenic effects.

With increased urbanization and greater unemployment and poverty, economic differentiation and associated problems, amounts of waste and wastewater volume will increase greatly in South Africa. This will result in a considerable challenge to solid and liquid waste treatment technologies and infrastructure to deal with increasing demands.

Research during the past decade or two, which has been promoted by the Water Research Commission and other institutions, has resulted in the acceptance of modified activated sludge systems as the standard procedure to remove phosphate from municipal wastewaters. It can be said with a considerable degree of certainty that, at most, only a marginal improvement in the phosphate removal capacity could currently be achieved by the manipulation of the biology of the system. The general method to achieve higher levels of phosphate removal is through the addition of chemicals such as ferric chloride to remove residual phosphate by precipitation. Such additions can be achieved by appropriate post treatment or in-process dosage of the chemicals. However, in the post treatment step, a tertiary separation stage of settling, flotation or filtration is required for the removal of the precipitated phosphate. In-process dosage has the disadvantage that the treatment works loses its biological phosphate removal capacity to some extent and also that relatively high concentrations of chemicals are needed. In both cases the entire effluent stream has to be treated.

There is an alternative approach which, in principle, is more attractive than the classical precipitation technique. This process employs crystallization technology and is designed to exploit the best characteristics of the chemical, physical and biological driving forces in an integrated system. Among the most important advantages of an integrated crystallization process are:

- Crystallization technology does not produce sludge as, e.g. with ferric chloride precipitation, which requires subsequent dewatering.

- The crystallized phosphate can be recycled directly to the phosphate industry.

- In contrast to the use of precipitating agents, no undesirable ions are introduced which can contribute to increased salination of rivers and impoundments.

- The introduction of crystallization technologies into existing works which, as a result of overloading or other reasons, do not meet the requirements for the phosphate standard, can extend their lifetime without major extensions to the works and ensure compliance with the current legislation. This advantage is also applicable to those works that do not meet the legislative standards for short periods of time.

- As many as 50% of the country's municipal wastewater treatment works currently employ biological filtration systems. Such systems only remove minimal amounts of phosphate. One of the unique advantages of in-process phosphate crystallization is that phosphate-rich filter effluents can be diverted partially or in toto to a suitably equipped process to achieve the removal of

nitrate and phosphate by activated sludge microorganisms and the crystallization stage. This can lead to considerable capital savings.

- In contrast with tertiary phosphate crystallization or precipitation, the integrated process requires treatment of a sidestream of the order of 10% of the total flow which has a major impact on the chemical demand and physical dimensions of the reactor. In the case of lime dosage, the main portion is required for achieving a pH increase which emphasises the benefit of using only a sidestream. Further reduction in reactor size can be achieved by the withdrawal of a sidestream with high phosphate concentrations which favours the crystallization kinetics. These advantages can be achieved because both the biological and the physical driving forces of the integrated process are exploited.

Research by the CSIR, in collaboration of the Water Research Commission, has already demonstrated the technological feasibility of the integrated process at laboratory scale (Momberg, 1993a). The pilot evaluation, conducted in collaboration with the City Council of Pretoria should contribute significantly to obtaining reliable design criteria leading to the full-scale implementation of phosphate crystallization technology.

1.3 PROJECT OBJECTIVES

The original objectives of the project were:

1.3.1 The construction and commissioning of a phosphate crystallizer at module 9 (13 Mℓ/d) of the Pretoria municipal activated sludge plant at Daspoort. The crystallizer will treat a side-stream from the anaerobic reactor of this plant, and the treated effluent from the crystallizer will be returned to the same plant.

1.3.2 To determine the capacity of the integrated crystallization and activated sludge system to limit phosphate concentrations under dynamic conditions to maximally 1 mg/ℓ (as P) in the final effluent.

1.3.3 To determine how much of a phosphate-rich trickling filter effluent can be added to an integrated crystallization/activated sludge system without exceeding the effluent standard of 1 mg/ℓ (as P) in the combined effluent.

1.3.4 Determination of the pretreatment, specifically clarification, of the crystallization side-stream that is required to ensure the successful operation of the crystallizer.

1.3.5 To determine the effect, if any, that the integration of the crystallization process may have on the ability of the activated sludge to accumulate and liberate phosphate.

1.3.6 To establish the critical design and operational aspects on which the successful commissioning and maintenance of the crystallizer will depend.

1.3.7 To compile guidelines for the implementation of a phosphate crystallizer in municipal wastewater treatment works.

1.3.8 To prepare a cost evaluation comparison between current processes and the crystallizer option.

1.4 ACHIEVEMENT OF OBJECTIVES

Problems and delays in the progress experienced during the course of the project, where beyond our control and resulted in concentrating the research efforts on the pilot-scale crystallization. No full-scale evaluation was conducted to operate the project more cost effectively. The effect of integration of the crystallizer into an activated sludge system was therefore also omitted as it was considered by the Steering Committee that this objective was of lesser importance and the probability of having a major influence on the performance of the activated sludge system would be small.

The limitations in the adaptability of the laboratory-scale crystallizer, especially at low flow rates, has resulted in scant data at low recycle ratios. However, the data were sufficiently reliable to provide design guidelines and insight into operational aspects for the successful implementation of the technology and maintenance of the crystallizer integrated into a municipal treatment works. Carbonate, at concentrations in excess of 2 mM in the effluent, interferes with the crystallization process. An acidification and degassing stage will therefore be required before adjusting the pH to approximately 10 for effective phosphate crystallization.

The total treatment costs, when degassing is employed, are of the order of R1,60 to R2,10 per m^3. However, only a sidestream of the total influent volume has to be treated to relieve the load on the biological phosphate removal process. This impacts on the economy of the technology, and the treatment costs under prevailing conditions, using sodium hydroxide for pH adjustment, would be approximately 10 to 21 cents/m^3, depending on the need to degas or not. The cost for degassing is therefore of the order of 50% of total treatment cost. Finally, the cost using either sodium hydroxide or calcium hydroxide for the process would be 21 cents/m^3 and 16 cents/m^3 respectively, when degassing is employed.

To establish the crystallization technology in South Africa, it will be necessary to further evaluate and collate performance data at pilot and full-scale to fine-tune the design of the crystallizer.

II. LITERATURE SURVEY

2.1 PROCESS HISTORY

Crystallization is an important separation process which can be used in a number of industries. In many cases crystallization offers an energy-saving method for separating an individual substance from a mixture of substances, e.g. sucrose, sodium chloride, fertilizer chemicals, and pharmaceuticals. The major purpose of crystallization technology is the production of a pure product (Myerson, 1990). Crystallization should aim at minimizing losses, which should not exceed the limit as determined by the required purity. A number of additional product specifications which may have to be met include crystal size distribution, storage characteristics, bulk density, filterability, slurry viscosity and dry solid flow properties (Nývlt, 1978). Based on such specifications it is necessary to select the proper process, equipment and operational regime.

Phosphate can be removed from effluents by crystallization. The chemistry of the system will be discussed in relative detail under sections 2.2 and 2.3. The crystallization process for this study centred around the formation of hydroxyapatite (HAP) from the activated sludge system. Of the many parameters of importance in the crystallization of phosphate, control of pH and the calcium concentration derived from the addition of lime, are of prime importance. The process of crystallization is generally encouraged by the introduction of a suitable seed material. To prevent the formation of a solid mass of calcium phosphate, fluidization of the seed support material is essential. Other parameters such as feed rate, fluidization velocity and hydraulic residence time, mixing to prevent supersaturation and the crystal mass:area ratio need to be considered for the successful implementation of phosphate crystallization technologies.

The technical feasibility of phosphate crystallization as a unitary process has been demonstrated (Joko, 1984; Kokobori & Kyosai, 1982; Momberg, 1993a; Momberg & Oellermann, 1992; Van Dijk & Braakensiek, 1984; Zoltek, 1974). Crystallization technology to obtain struvite has also been investigated (Momberg, 1993b; Momberg & Oellermann, 1992). It has found application in ponding systems (Moutin *et al.*, 1992), softening of drinking water and heavy metal removal from industrial wastewater (Van Dijk & Wilms, 1991).

The first application of crystallization was the softening of drinking water in which limestone ($CaCO_3$) pellets are formed. In the early 1970's a softening process was developed at the Municipal Treatment Works of Amsterdam and patented by DHV Consultants, who are responsible for the commercialization of the Crystalactor® pellet reactor (Eggers *et al.*, 1991a, Janssen *et al.*, 1991). During the past 15 years, some 20 plants have been installed in The Netherlands and 15 plants elsewhere in Europe.

The second application was the removal of phosphate from wastewater in which hydroxyapatite [$Ca(PO_4)_2$] pellets are produced. Over a period of ten years, DHV Consultants have developed this process from pilot to a full-scale plant at Westerbork, The Netherlands (Van Dijk & Wilms, 1991).

Immobilization of phosphate could be achieved in a combined process in which the known potential of microorganisms to concentrate phosphate could be used in tandem with a crystallization reactor in which a side-stream of the phosphate enriched water could be treated. Typical phosphate influent concentrations of 10 mg P/ℓ are easily increased to 50 mg P/ℓ as a consequence of phosphate released during the anaerobic phase of biological wastewater treatment. By increasing the pH, the formation of HAP is favoured whereby a final phosphate concentration of less than 1mg/ℓ can be achieved. This makes it feasible to treat only a relatively small proportion of the entire incoming stream to effectively decrease the incoming load of phosphate, thereby relieving the pressures on the biological phosphate removal process. This would ensure that the effluent discharge standard for phosphate is achieved all the time.

2.2 THE THERMODYNAMICS OF THE Ca-Mg-PO_4-CO_3 SYSTEM

Table 2-1 lists some of the possible solid compounds which may arise from a system containing calcium, magnesium, phosphate and carbonate ions which commonly occur in effluents. The diversity of solids possible gives a hint at the complexity of the system under consideration. Prominent solids containing the above four ions, and including one other, such as fluoride, or potassium, have also been included in the list.

The thermodynamics of the four major crystalline species in the precipitation of calcium phosphate has been discussed in detail (Momberg, 1993a). An overview of the subject is presented below.

2.2.1 Effect of temperature

Very little work has been done on this aspect. Most workers have concentrated on measuring thermodynamic data at 25° C, the standard temperature, and at 37° C, the temperature of the human body. These studies focused on models of bone and tooth growth, and the formation of dental caries.

The following additional thermodynamic constants, namely the free energy change upon forming the solid (ΔG), the enthalpy change (ΔH) and the entropy change (ΔS) have been measured. The free energy of formation relates to the formation constant as

$$\Delta G = -RT\ln K = -2{,}303RT\log K$$

The ΔH can be used to convert the log of the solubility product (K_{sp}) at 25° C to an approximation of the logK_{sp} at temperatures below 100° C. The Δlog K gives the increase in log K_{sp} for every 10° C rise in temperature, and is derived from the equation

$$\log K(T_2) - \log K(T_1) + \frac{\Delta H}{2.303\,R}\left(\frac{1}{T_1} - \frac{1}{T_2}\right)$$

where T_1 and T_2 are the temperatures of interest in Kelvin, and the gas constant, R = 8,314x10^{-3} kJ/Kelvin.Mole.

Table 2-1. Prominent solids occurring in the Ca-Mg-PO_4-CO_3 system. The first four listed are the most important in phosphate removal (Wade *et al.*, 1993)

Name	Abbreviation	Formula
Amorphous Calcium Phosphate	**ACP**	**$Ca_3(PO_4)_2.xH_2O$**
Octacalcium Phosphate	**OCP**	**$Ca_8(HPO_4)_2(PO_4)_4.5H_2O$**
Brushite	**DCPD**	**$CaHPO_4.2H_2O$**
Hydroxyapatite	**HAP**	**$Ca_5(PO_4)_3(OH)$**
Monetite	DCPA	$CaHPO_4$
Whitlockite	TCP	$Ca_3(PO_4)_2$
Monocalcium Phosphate	MCP	$CaH_4(PO_4)_2.H_2O$
Fluorapatite	FAP	$Ca_5(PO_4)_3F$
Magnesium Hydroxyapatite	MAP	$Mg_5(PO_4)_3OH$
Newberyite		$MgHPO_4.3H_2O$
Hydrated Trimagnesium Phosphate	HTMP	$Mg_3(PO_4)_2.22H_2O$
Bobierrite		$Mg_3(PO_4)_2.8H_2O$
Potassium Magnesium Phosphate	PMP	$MgKPO_4.6H_2O$
Trimagnesium Phosphate	TMP	$Mg_3(PO_4)_2$
Struvite		$MgNH_4PO_4.6H_2O$
Magnesium Fluorapatite	MFAP	$Mg_5(PO_4)_3F$
Wagnerite		Mg_2PO_4F
Aragonite		$CaCO_3$
Calcite		$CaCO_3$
Dolomite, ordered		$CaMg(CO_3)_2$
Dolomite, disordered		$CaMg(CO_3)_2$
Magnesite		$MgCO_3$
Nesquehonite		$MgCO_3.3H_2O$
Lansfordite		$MgCO_3.5H_2O$
Hydromagnesite		$Mg_4(CO_3)_3(OH)_2.3H_2O$

2.2.2 Effect of pH

The pH is the most important parameter controlling the chemistry of the Ca-Mg-PO_4-CO_3 system.

HAP crystallizes onto the surface of seed material such as phosphate rock, according to the following equation (Hirasawa & Toya, 1990).

$$5Ca^{2+} + 3HPO_4^{2-} + 4OH^- = Ca_5(PO_4)_3(OH) + 3H_2O$$

It is therefore expected to predominate at high pH, where there is a higher concentration of hydroxide ions.

DCPD crystallizes according to the general equation

$$Ca^{2+} + H^+ + PO_4^{3-} = CaHPO_4.2H_2O$$

It is therefore expected to predominate at low pH, where there is a higher concentration of H^+ ions.

Although HAP is the thermodynamically most stable solid under many conditions, it becomes less stable than DCPA and DCPD at reduced pH. A calcium phosphate solid exposed to a solution more acid than the point at which two solids are in equilibrium with the solution may be covered with a surface coating of a more acidic calcium phosphate. This surface phase might persist for some time, since calcium phosphate solutions are generally dilute, and solubilities low. Apparent solubility behaviour will then be quite different from the solid exposed to the solution (Brown, 1973), a fact which may have led workers to believe that the properties of calcium phosphate solids, HAP in particular, are quite variable (Deitz *et al.*, 1964; LaMer, 1962; Rootare *et al.*, 1962).

2.2.3 Supersaturation

The concept of supersaturation is fundamental to understanding calcium phosphate precipitation.

The ionic activity product (IAP) is defined as the product of all the concentrations of species comprising the solid, raised to the powers of their stoichiometries, e.g. for $Ca_5(PO_4)(OH)$ the IAP would be: $[Ca^{2+}]^5[PO_4^{3-}]^3[OH^-]$, where the square brackets are the molar concentrations of the species within.

When the IAP of a solid is greater than the solubility product (K_{sp}) of the solid, the solution is said to be *supersaturated* with respect to that solid.

The solubility of a compound is calculated as the saturation index (SI), defined as the ratio of the IAP to the K_{sp}. It is most conveniently represented as the logarithm:

$$\log\ (Saturation\ Index) - \log\ SI - \log\left(\frac{IAP}{K_{sp}}\right)$$

For example, for HAP ($Ca_5(PO_4)_3(OH)$), the log SI index would be:

$$\log SI = \log\left(\frac{[Ca]^5[PO_4]^3[OH]}{K_{sp}}\right)$$

A log SI of zero means that the IAP of the solid species is exactly equal to the solubility product, and therefore the species exists in solution at its saturation limit. If a potential solid has a negative log SI, it is undersaturated, and will never precipitate, and if it has a positive log SI, it is supersaturated, and will precipitate over a period determined by the kinetics of the precipitation process.

The supersaturation ratio, S, which accounts for the number of ions present in the solid, is defined as

$$S = \left(\frac{IAP}{K_{s_p}}\right)^{\frac{1}{n}}$$

where IAP is the ionic activity product, and K_{sp} is the solubility product; n is the number of ions in the neutral molecule (n = 10 for HAP). This quantity allows for better comparison between supersaturation of various solids in solution.

The relative supersaturation index, σ, which accounts for the number of ions present in the solid, is defined as

$$\sigma = \left(\frac{IAP}{K_{s_p}}\right)^{\frac{1}{n}} - 1$$

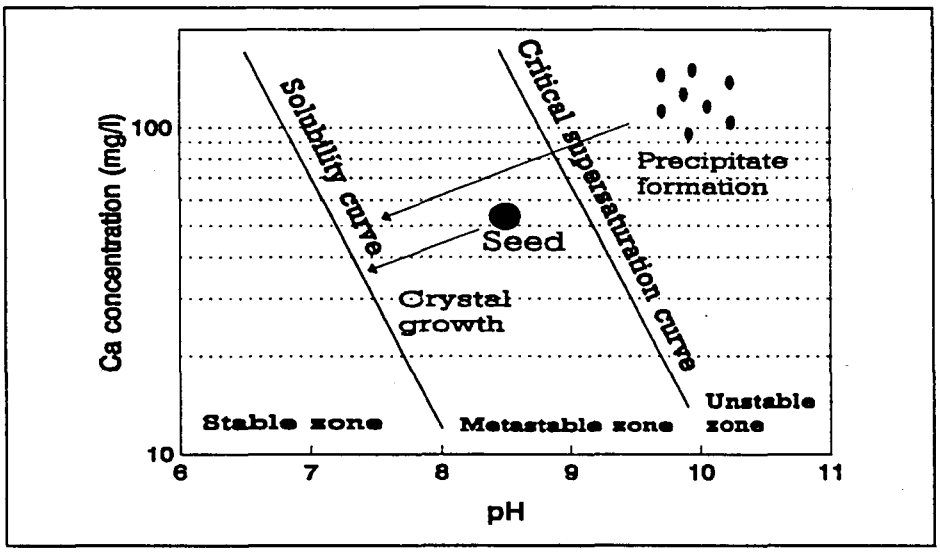

Fig. 2-1. Stability zones of calcium phosphate

2.2.4 Metastability

Metastable solutions are supersaturated and Joko (1984) developed a series of critical supersaturation curves for various concentrations of calcium phosphate. These curves represent limits of supersaturation above which spontaneous precipitation occurs. The metastable zone of calcium phosphate is defined as the region between the solubility curve and the critical supersaturation curve (Fig. 2-1). In this region calcium phosphate solids do not precipitate by addition of calcium hydroxide, but they may crystallize out on the surface of seed crystals. The unstable zone above the critical supersaturation curve is the range where a spontaneous precipitation reaction takes place, and the phosphate concentration decreases to a level determined by the solubility curve.

2.2.5 Effect of ionic strength

Not much work has been done on the effects of ionic strength on the precipitation of calcium phosphates. However, Rootare *et al.* (1962) reported that the activity product calculated for HAP was not constant but varied widely with the ratio of solid:water. The solubility was less when more of the solid had been dissolved. An increase in ionic strength by "spectator" ions, such as NaCℓ, leads to a *decrease* in solubility of HAP. This "salting out" effect observed by addition of NaCℓ at constant slurry density is not general. The increase in ionic strength resulting from the use of different slurry densities alone enhanced the solubility, which is the more common "salting in" effect. It is likely that the researchers were obtaining interference from supposedly inert Na and Cℓ ions with the growth of intermediate solids. It is mentioned that the molar ratio of calcium to total phosphate in the extracts was not constant at the HAP level (1,667), but approached this value as a large fraction of the material dissolved, which suggests that minerals other than HAP were controlling the solution composition.

In general, ionic strength affects the "activities" of ions in solution, and this, in turn, affects the formation constants of compounds e.g. solids.

2.2.6 Interfering ions

Fluoride (F^-) significantly enhances phosphate removal from solution in concentrations of over 10^{-5} M (Meyer & Nancollas, 1972). Fluoride readily substitutes for OH^- in HAP and has almost the same effect as a pH increase on its solubility. FAP is formed, which is more stable than HAP (Nancollas & Tomažič, 1974).

The precipitation of $CaCO_3$ removes Ca from solution and thus retards the precipitation of calcium phosphate solids. Ferguson *et al.* (1970, 1973) suggest that bicarbonate ions cause an increase of phosphate concentrations in solution in the pH range from 9,0 to 10,5 because of competitive precipitation of $CaCO_3$, which removes free calcium from the system, causing less calcium phosphate to precipitate. Joko (1984) reports that increased alkalinity reduces phosphate removal effectively in batch experiments, but there was no difference in phosphate removal in continuous flow experiments with alkalinity between 50 and 250 mg/ℓ. It was therefore stated that phosphate removal is more strongly affected by pH than by alkalinity. Presumably this indicates that some kinetic control of the formation of calcium carbonate with respect to calcium phosphates is possible.

Magnesium competes thermodynamically with calcium for phosphate ions. Mg was introduced into precipitation experiments at 25° C, with solutions of medium (Ca = P = 50 mM; Ca + Mg = P = 50 mM) and low (Ca = P = 10 mM; Ca + Mg = P = 10 mM) concentrations (Abbona *et al.*, 1992). The solids occurring one year later were DCPD in the more concentrated solutions, and HAP and a mixture of whitlockite and newberyite, with the general formula $Ca_9MgH(PO_4)_7$ in the others.

2.2.7 Optimum Ca:P ratio

It is tempting, on the basis of different Ca:P ratios in the calcium phosphate solids, to attempt to precipitate the different solids by modifying the Ca:P ratio of the bulk solution. However, at a Ca:P = 1,333, the ratio found in OCP, and at a controlled ionic strength of 0,10 the precipitation of OCP appears to be limited to a pH range of 6 - 7 (de Rooij *et al.*, 1984). At pH 5,0 DCPD was formed at all levels of supersaturation, whereas at pH 5,5 it occurred only at high supersaturation, with OCP precipitating at low supersaturation. At higher pH (7,4 and 8,0) the results point to the formation of a HAP-like material.

Nancollas *et al.* (1979) precipitated calcium phosphates from solutions (pH 7,4; 37° C) and with Ca:P ratios of 1,45 and 1,33 OCP and HAP precipitate. At a Ca:P ratio of 1,00 OCP and DCPD precipitate.

Thus it can be seen that for the same Ca:P ratio, different solids precipitate at different pH values. In the light of the fact that HAP is the most stable solid over the pH range greater than 4, it is apparent that the precipitation reactions are under kinetic control.

2.3 KINETICS OF THE Ca-Mg-PO_4-CO_3 SYSTEM

2.3.1 Crystal formation, growth and dissolution

Crystal formation occurs in two stages, viz. nucleation and growth.

Nucleation is the generation of microcrystals from solution, and *growth* is the process whereby ions are transported to the surface, oriented and incorporated into the crystal lattice. When both nucleation and growth occur simultaneously (as in unseeded supersaturated solutions) homogeneous nucleation results. Under these conditions, the crystals tend to be small and finely dispersed, and may exist as flocs. When growth is dominant (as in solutions of low supersaturation), larger and fewer crystals result, tending to grow on surfaces in a process known as heterogeneous nucleation (Van Dijk & Wilms, 1991).

2.3.1.1 Precipitation curves

The kinetics of precipitation at high pH can be divided into four stages (Jenkins *et al.*, 1972), which is presented as an idealized scheme in Fig. 2-2.

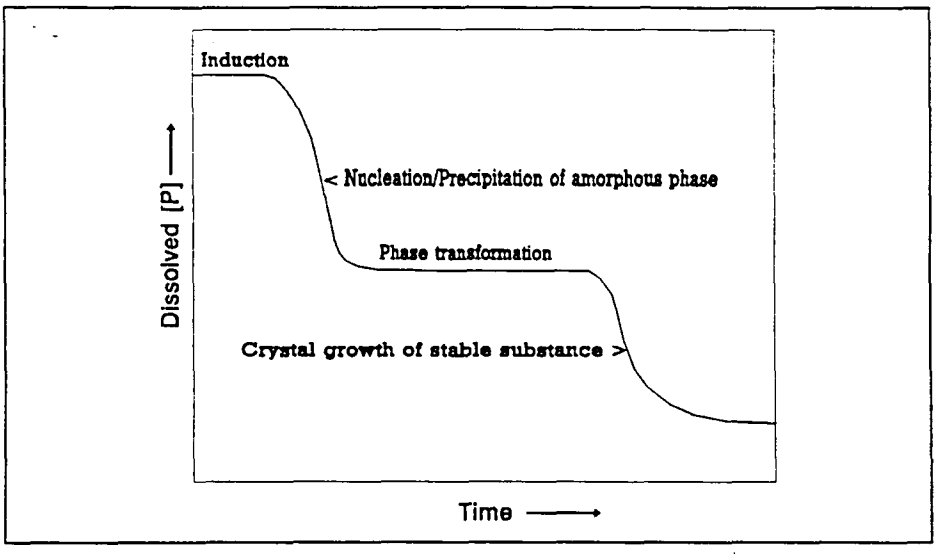

Fig. 2-2. Idealized scheme for calcium phosphate crystallization kinetics

- A period of induction before any measurable decrease in dissolved phosphate.
- Formation of a metastable precipitate and removal of phosphate from solution.
- Phase transformation from metastable precipitate to a more thermodynamically stable solid - no net phosphate removal.
- Crystal growth at the expense of the metastable solid and solution components - more phosphate removed from solution.

The length of the stages depends on pH, reagent concentration, temperature, presence of interfering ions and presence of preformed nuclei (Jenkins *et al.*, 1972). In summary, factors affecting lag times (hence metastability of dissolved calcium phosphate) are as follows:

- Temperature
- pH
- Ca:P ratio
- Ionic strength
- Other ions.

2.3.1.2 Rate laws

The rate of crystal formation is usually proportional to some power of the supersaturation.

Zoltek (1974) presents a general empirical growth equation:

$$\frac{dC}{dt} = -k \frac{A}{V} (C - C_0)^n$$

where

$^{dC}/_{dt}$ = the rate of change in concentration C as a function of time;
C is the concentration of the limiting reagent;
C_0 is the equilibrium concentration;
k is the rate constant;
A is the surface area of the growing crystal;
V is the liquid volume surrounding the crystals; and
n is the order of the reaction.

For precipitation of very insoluble solids, such as from the calcium phosphate system, the term C_0 is negligible. It was found that for calcium phosphate growth on phosphate rock seed crystals, the initial phase of growth is described by n varying from 7 to 13 for different initial conditions. Zoltek (1974) reports an average value of n of approximately 1,9 for steady state growth. Ferguson *et al.* (1973) report a value of n = 2,7 for calcium phosphate deposition from activated sludge. Zoltek (1974) found that the rate constant is a function of pH, with an increase in the logarithm of the rate constant of 0,34 per unit increase in pH. This means that there is approximately a two-fold increase in k for each unit increase in pH. It is suggested that this increase is as a result of the increasing supersaturation ratio.

Marshall & Nancollas (1969) studied the kinetics of crystal growth on well-characterized DCPD seed crystals in supersaturated calcium phosphate solution (T_{Ca} = 4,37 mM; T_P = 10,50 mM). Crystal growth proceeded immediately upon inoculation with seed crystals, and the rate curves are consistent with the kinetic equation

$$Rate\ of\ crystal\ growth = \frac{dT_{Ca}}{dt} = -ksN^2$$

where k is the specific rate constant for growth, s is a term proportional to the number of DCPD growth sites, and N is the number of moles of DCPD to be precipitated before equilibrium is reached, i.e. N is the supersaturation of DCPD in the system. To paraphrase, the rate of crystal growth of DCPD is second-order with respect to the supersaturation of DCPD. The rate of crystallization was independent of fluid dynamics, and the activation energy of 48,9 kJ/mol indicates a surface-controlled process. The crystallization of a number of other 2-2 symmetrical electrolytes has been shown to follow the same kinetic equation (Nancollas *et al.*, 1979).

For calcite ($CaCO_3$), the rate of crystallization is proportional to the square of the supersaturation (Nancollas *et al.*, 1983). Addition of magnesium inhibits crystallization of calcite, but not wagnerite or aragonite. Magnesium has a partition coefficient between calcite and solution of 0,028, implying that it is strongly adsorbed to calcite. It is probably disrupting calcite growth through adsorption to growth sites.

The form of the rate laws is derived largely from identification of the slowest step in a sequence of reactions. Overman *et al.* (1983) developed a kinetic model for the fixation of phosphate in a reactor according to the following scheme:

Adsorption/Desorption

$$P + Q \underset{k_d}{\overset{k_a}{\rightleftharpoons}} A \qquad k_a = 3{,}0\ min^{-1};\ k_d = 0{,}25\ min^{-1}$$

Forward/Backward Transformation

$$A + S \underset{k_b}{\overset{k_f}{\rightleftharpoons}} B + Q \qquad k_f = 0{,}09\ min^{-1};\ k_b = 0{,}03\ min^{-1}$$

Decomposition and Reaction

$$B \underset{k_r}{\overset{k_s}{\rightleftharpoons}} P + S \qquad k_s = 0{,}065\ min^{-1};\ k_r = 0{,}00098\ min^{-1}$$

$$B \downarrow \rightarrow F + S$$

Thus it can be seen that *adsorption* is an important component of the mechanism of crystal formation, and *desorption* is an important component of crystal dissolution.

2.3.1.3 Directional blocking of growth

Thomas (1991) studied the effects of the Mg^{2+}, Ba^{2+}, Pb^{2+}, Sr^{2+}, F^- and $C\ell^-$ ions on the stabilization and conversion of ACP to HAP at 298 K and pH = 9,00. The order of stabilization of ACP is $Mg^{2+} > Ba^{2+} > Sr^{2+} > Pb^{2+} \sim F^- \sim C\ell^-$. Mg^{2+} appears to block the growth of HAP crystals in the 001 direction, while other ions do not show such directional blocking effect.

2.3.2 Ostwald's rule of stages

Often the precipitation reactions are under kinetic control. This means that under the conditions of crystallization, the formation of one solid is slow, allowing precipitation of a less stable solid. It has been shown that an empirical generalization, known as the "Ostwald Rule of Stages" (Ostwald, 1897 cited by Wade *et al.*, 1993) applies to this system. This rule states simply that:

When a number of similar solids are highly supersaturated, the least stable solid will precipitate first .

This is qualitatively understood if one considers that an efficiently, tightly packed crystal will tend to be the most stable form. The alignment of atoms necessary to achieve efficient tight packing in the crystal will be more time-consuming than that for a more loosely-packed (and hence less stable) form. This condition is in direct conflict with the thermodynamic driving force to achieve the most stable arrangement. However, once

formed, these less stable solids gradually convert to the thermodynamically more stable forms, and ultimately to the most stable crystal.

HAP is the thermodynamically most stable solid. Following the Ostwald empirical rule one might expect the least stable solid to precipitate first, and experience has shown that the two hydrated salts, OCP and DCPD, are the ones that precipitate most easily, particularly at ambient temperatures (Brown, 1973).

Heughebaert *et al.* (1986) studied the crystallization of calcium phosphate solids from metastable supersaturated solutions (25°C; pH 6,00) following seeding with well characterized OCP. At low supersaturation ($\sigma < 1{,}02$), OCP was grown, whereas at higher supersaturation, DCPD nucleates and grows on the OCP seed.

A study by van Kemenade & De Bruyn (1987) with unseeded calcium phosphate solution shows that calcium phosphate precipitates according to Ostwald's rule of stages. At low pH (below the OCP/DCPD thermodynamic crossover point) OCP crystallizes first, and then converts to DCPD, and eventually to HAP.

There are several examples of kinetic control of seeded precipitation and secondary nucleation (Nancollas & Tomažič, 1977). The kinetics of crystal growth of DCPD was studied by seeded precipitation and in the absence of induction effects. In solutions in which DCPD and HAP are both supersaturated, the addition of HAP seed crystals induces precipitation of DCPD on the HAP surface, although the HAP is thermodynamically more stable.

At higher pH ACP precipitates first, converts to OCP and finally to HAP. TCP is not important in systems such as these.

The processes may be summarized:

low pH:	$Ca^{2+}_{(aq)} + PO_4^{3-}_{(aq)} \rightarrow$ OCP $\rightarrow$ DCPD $\rightarrow$ HAP
around neutral pH:	$Ca^{2+}_{(aq)} + PO_4^{3-}_{(aq)} \rightarrow$ OCP + DCPD $\rightarrow$ HAP
high pH:	$Ca^{2+}_{(aq)} + PO_4^{3-}_{(aq)} \rightarrow$ ACP $\rightarrow$ OCP $\rightarrow$ HAP

2.3.3 Homogeneous versus heterogeneous nucleation

The higher the supersaturation levels, the more applicable is the Ostwald rule, i.e. the more supersaturated the solution, the more likely the less stable forms will occur. Also, the more supersaturated the solution, the greater the potential for *homogeneous* nucleation, which is the spontaneous formation of crystals in the solution bulk, which are often internally quite disordered, due to the rate at which they form. Homogeneous nucleation can result in micro-crystals being formed which remain suspended. Due to the high rate of formation of the crystals, they can be quite fragile, and thus more easily eroded to produce suspended solid particles.

Conversely, at low supersaturation, *heterogeneous* nucleation is favoured, which occurs in a more reproducible way, and in which the crystals formed are much more ordered. Heterogeneous nucleation takes place on available surfaces (e.g. suspended sand particles). The crystals tend to be large, and fairly robust, thus unlikely to disintegrate, and to be a source of suspended solids.

Ferguson *et al.* (1973) state that 85-90 % of dissolved phosphate may be removed in a recycling reactor (in which precipitated solids are contacted with fresh supersaturated solution - heterogeneous nucleation) at pH 8,0.

Several practical measures can be taken to prevent homogeneous nucleation of ACP at high pH (Eggers & Van Dijk, 1986; Van Dijk & Braakensiek, 1984):

- Intensive mixing of caustic soda or lime (applied as a pure solution) to avoid local high supersaturation.
- Dosing with caustic soda in more than one step.
- Recirculation of effluent.
- Mixing of caustic soda or lime with grains of high specific surface area.

2.3.4 Effect of various parameters on crystallization

2.3.4.1 The effect of pH

Brown (1980) studied calcium phosphate precipitation by measuring the decline in phosphate concentration resulting from the reaction between dilute orthophosphate and aqueous calcitic limestone suspensions. The rate of phosphate disappearance from solution increased with an elevation of pH at 7,0 to 8,4.

Zoltek (1974) found that for calcium phosphate growth on phosphate rock seed crystals, the rate constant is a function of pH, with an increase in the logarithm of the rate constant of 0,34 per unit increase in pH. In other words, there is approximately a two-fold increase in k for each unit increase in pH. It is suggested that this increase is as a result of the increasing supersaturation ratio. Both the PO_4^{3-} and OH^- concentrations increase logarithmically with increasing pH.

In neutral and acidic solution, DCPD has been found to be the first crystalline solid to precipitate. There is also the additional possibility of an unstable amorphous solid as a precursor (Zhang *et al.*, 1992). However, at pH 7,4, although the formation of DCPD is expected to precede that of OCP in accordance with the Ostwald rule of stages, most studies fail to detect DCPD in the transformation from ACP to OCP (van Kemenade & de Bruyn, 1987). DCPD has relatively rapid growth and dissolution kinetics, compared with other calcium phosphate solids and will probably be important in governing the composition of the surrounding solution.

Zhang *et al.* (1992) studied the kinetics of dissolution of DCPD and of nucleation of OCP (37°C; pH 7,0-7,4). Relative supersaturation, σ, with respect to DCPD and OCP crystals is defined as:

$$\sigma(DCPD) = \left(\frac{[Ca^{2+}][HPO_4^{2-}]}{K_{sp}(DCPD)}\right)^{\frac{1}{2}} - 1$$

$$\sigma(OCP) = \left(\frac{[Ca^{2+}]_4[H^+][PO_4^{3-}]_3}{K_{sp}(OCP)}\right)^{\frac{1}{8}} - 1$$

Supersaturation of DCPD varies with respect to $[H^+]^{0.5}$, whereas supersaturation of OCP varies with respect to $[H^+]^{0.125}$. This means that as pH increases, the $[H^+]$ will decrease, and the supersaturation of DCPD will diminish faster than that of OCP.

The established pH dependence of growth and dissolution kinetics of various calcium phosphate solids suggests that the marked difference in induction periods at pH 7,00 and 7,40 is primarily a consequence of acidity, rather than small differences in thermodynamic driving force (Zhang *et al.*, 1992).

2.3.4.2 Supersaturation

Zoltek (1974) remarked that a typical municipal effluent has 40 mg/ℓ Ca and 10 mg/ℓ P, and a pH of 7,5. The supersaturation ratio of HAP in such a stream is 12,6. Spontaneous precipitation of HAP does not occur due to kinetic factors. Thus there is a limit of supersaturation below which a solution will not precipitate solids.

The supersaturation ratio of calcite can be as high as 3,1 without spontaneous homogeneous nucleation of calcite whereas it nucleates heterogeneously at a supersaturation ratio of 1,5. Thus the supersaturation ratio does not need to be so high for heterogeneous precipitation (Reddy & Nancollas, 1971).

According to Nancollas & Wefel (1972) the kinetics of growth of DCPD shows a second order dependence of rate on supersaturation, and dissolution is first order with respect to undersaturation. So the rate of reaction is dependent on supersaturation in this case.

In precipitation of calcium phosphates at 37° C from solutions with pH of 5,0 to 11,0 it was noted that, despite the fact that the supersaturation of HAP, OCP, and DCPD are often in the order HAP >> OCP >> DCPD, DCPD nucleates more easily than OCP and HAP at low pH, while OCP nucleates more easily than HAP at median to high pH (Boistelle & Lopez-Valero, 1990). These facts cannot be explained by the differences in the surface free energies of the solids. It was suggested that the values of the kinetic coefficients change as a function of the concentration. In the proposed model, the kinetic coefficients of OCP and HAP are smaller than that of DCPD by 10 and 18 orders of magnitude at pH = 6,5. These differences reduce to 3 orders of magnitude at pH = 10,0. Accordingly, nucleation of OCP and HAP is favoured with increasing pH. The implication that the coefficients are dependent on the supersaturation levels is revolutionary, and it is much more likely that the proposed mechanism resulting in the rate law has omitted a step in which the supersaturated species is important.

2.3.4.3 Ionic strength

Not much work has been done in this field, researchers preferring to remain at or near physiological ionic strength. However, Termine & Posner (1970) established a dependence of metastability on ionic strength. As the ionic strength of the solution increases, so does the lag time. Assuming the "spectator ions" which are modifying the ionic strength are not behaving as interfering ions, the implication is that increased ionic strength stabilizes ACP in the solution phase.

2.3.4.4 Ca/P ratio

Termine & Posner (1970) established that, as the Ca:P ratio decreases, the lag time (t_l) increases.

2.3.4.5 Seeding surfaces

Jorgenson *et al.* (1973) found that phosphate removal by precipitation from waste water was more efficient than precipitation from pure solutions. Presumably this is due to the availability of particles which might act as seeding surfaces for precipitation of calcium phosphate.

Different seeding surfaces have vastly different effects on precipitation of calcium phosphates.

The deposition of calcium phosphate onto seeding surfaces has been extensively studied (Koutsoukos *et al.*, 1980; Nancollas & Wefel, 1976; Tomažič & Nancollas, 1975). In general, at low supersaturation, nucleation will be induced by the substance itself, or a closely matched foreign material, whereas at high supersaturation a large variety of foreign materials will act effectively as seed crystals (Joko, 1984). The effect of seed crystals on the kinetics of crystallization is shown in Fig. 2-3.

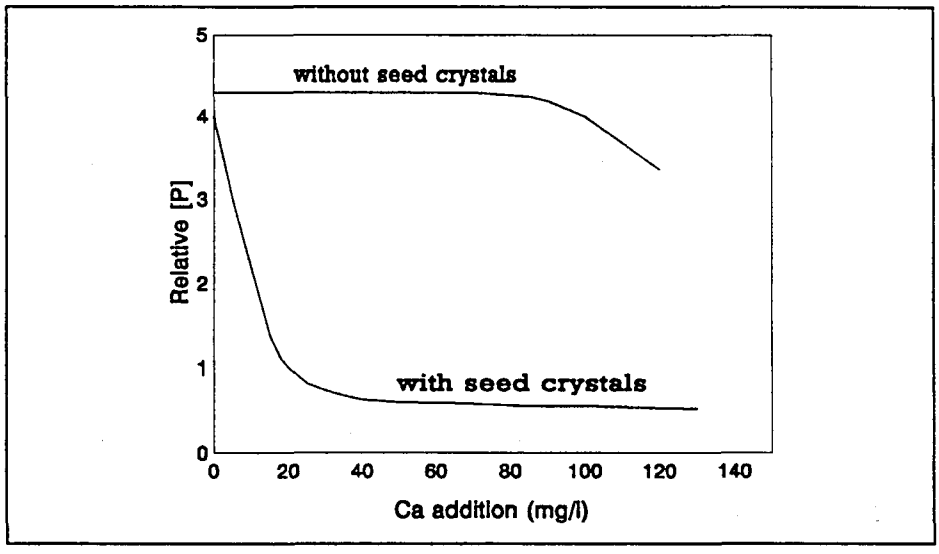

Fig. 2-3. Effect of seed crystals on phosphate precipitation

Quartz sand was found to be a good seed material. Although phosphate rock or bone charcoal were also shown to act as good seeding materials, they are easily affected by bicarbonate alkalinity, which reduces phosphate removal efficiency (Zoltek, 1974).

A solids recycle in a crystallizer significantly reduces the lengthy induction period, while a subsequent addition of preformed crystalline solids to supersaturated solutions eliminates the induction period of the amorphous precipitation, as well as the phase transformation (Jenkins *et al.*, 1972). In this case the time taken to reduce phosphate concentration by 80% was reduced from 100h to 16h. A residence time of 42 to 47 min

is sufficient to allow for a high degree of reduction of dissolved phosphate. A very high concentration of Ca^{2+} in solution was found to lengthen the induction period. Kaneko & Nakajima (1988) investigated the kinetics of phosphate removal from a solution containing 3,5 mg P/ℓ by seeding with various crystals. Equilibrium is reached in 40 to 45 h. Magnesia clinker, bone charcoal and zirconium hydroxide were the best seed crystals, whereas pumice stone was the poorest. The superior phosphate removal of the magnesia clinker seems to relate to the accompanying release of a small amount (~10mg/ℓ) of Mg^{2+} into the solution (Bischoff & Fyfe, 1968; Ferguson & McCarty, 1971; Smith & Hwang, 1978). The rate of crystallization was increased by pretreatment of the magnesia clinker with calcium chloride solution. This clinker is termed "activated" by the $CaC\ell_2$. Smith & Hwang (1978) proved that phosphate was removed from solution by adsorption.

If calcium phosphate is introduced as a seeding material either as HAP or TCP, amorphous precipitation products are obtained which transform slowly to crystalline compounds. Residual concentrations of about 0,2 mg P/ℓ are obtainable depending on the pH of the solution. The process is strongly retarded if carbonate or Mg^{2+} ions are present in the water.

If calcite is used as a seeding material, no retardation of the phosphate removal by CO_3^{2-} or Mg^{2+} is observed. Residual phosphate concentration depends only on the pH of the water and its calcium content.

Barone & Nancollas (1978) investigated the kinetics of growth of calcium phosphate on synthetic HAP, human enamel, whole dentine and human calculus (37° C; pH 7,97-5,10). Following an initial induction period, DCPD crystallization took place on all surfaces even though the solutions were highly supersaturated with respect to HAP. The second order crystal growth kinetics were characteristic of the crystallization of DCPD on pure DCPD seed material. The ability of the surfaces to nucleate DCPD fell in the order:

Synthetic HAP > enamel > calculus > dentine.

Nancollas & Wefel (1976) initiated a kinetic and microscopic study of the effectiveness of the calcium phosphate solids in nucleating, stable, saturated solutions of calcium phosphate (T_{Ca} = 0,005 M; T_P = 0,01 M). At low pH of 5,6 the solution, which was supersaturated in HAP and DCPD, was seeded with DCPD crystals. The crystals which grew had a Ca:P ratio of 1,0 which is characteristic of DCPD. Seed crystals of OCP, TCP and HAP were effective nucleators of DCPD under conditions in which DCPD was the dominant solid. The crystals grew according to second order kinetics, characteristic of DCPD growth. TCP was the least efficient nucleator, DCPD growth occurring only after an initial induction period. In all instances, the rate of DCPD growth was proportional to the square of the supersaturation, and the reaction was surface controlled. Scanning electron microscopy showed an amorphous or microcrystalline precursor to the development of the characteristic platelets of DCPD.

At physiological pH 7,4 the calcium phosphate system (T_{Ca} = 0,0014 M; T_P = 0,0008 M) was supersaturated with respect to all five calcium phosphate solids, viz. ACP, DCPD, OCP, TCP and HAP. Only OCP and HAP seed crystals were effective nucleators. The efficiency of OCP as a nucleator added further evidence for its

participation in the precipitation of HAP under these conditions (Nancollas & Wefel, 1976).

In the 60-80° C range and in acidic medium, the precipitation of either OCP or DCPD or DCPA onto DCPA seed occurs (Freche & Heughebaert, 1989).

From a series of porous ceramics based on HAP containing metal oxides, it was found that only those containing ZrO_2 stabilized with 8% YO_2 were able to induce calcium phosphate precipitate formation (Dalas & Koutsoukos, 1989).

Materials found to be good seeding materials for phosphate removal from solution are presented in Table 2-2.

Table 2-2. Seed material evaluated for phosphate removal

Seed Material	Quality	Reference
Quartz sand	Good	Zoltek (1974)
Phosphate rock	Fair	Zoltek (1974)
Bone charcoal	Fair	Zoltek (1974)
Bone charcoal	Good	Kaneko & Nakajima (1988)
Magnesia clinker	Very good	Kaneko & Nakajima (1988)
Zirconium hydroxide	Good	Kaneko & Nakajima (1988)
Pumice stone	Poor	Kaneko & Nakajima (1988)
Ceramics (most)	Poor	Dalas & Koutsoukos (1989)
Crystalline calcium phosphate	Good	Various

2.3.4.6 Temperature

It is a general rule of thumb that the rates of chemical processes approximately double for every 10° C rise. The kinetics of DCPA, growth onto DCPA was studied in the 60-80° C range and in acidic medium (Freche & Heughebaert, 1989). At 70° C the rate constant is small, and the order of the reaction is 4. At 80° C the rate of growth is higher and the order of the reaction is 2. The fact that the order of the reaction is changing means that the mechanism of the reaction is changing as the temperature is raised. Since rate laws are largely dependent on the slowest step in a sequence of reactions, it is likely that the rate constant for the slowest step increased at a greater rate than that of another step, causing the latter to become the slowest step. It was established that the rate of crystallization increases both as a function of temperature and supersaturation whereas the induction time of crystallization decreases both as a function of temperature and supersaturation.

2.3.4.7 Interfering ions

Table 2-3. The effects of interfering ions on various processes occurring in the calcium phosphate system

Substance	Effect	Process affected
Mg	Stabilization	ACP on HAP
Mg	Inhibition	ACP to crystalline transformation
Mg	Inhibition	ACP1 to ACP2 transformation
Mg	Inhibition	ACP2 nucleation
Mg	Inhibition	OCP growth
Mg	Increase	OCP induction period (> 10^{-3} M)
Mg	Blocking	HAP growth in one crystal growth direction
Mg	Inhibition	calcite formation
Mg	Stabilization	TCP structure by incorporation
$P_2O_7^{4-}$	Inhibition	DCPD growth
$P_2O_7^{4-}$	Blocking	HAP growth
Proteins	Inhibition	HAP growth and ACP dissolution
Citrate	Inhibition	ACP formation
Polyacrylate	Inhibition	ACP formation and transformation
EDTA	Inhibition	ACP formation
Casein	Inhibition	ACP transformation
Protein-polysaccharides	Inhibition	ACP formation only at high initial supersaturation
Polyphosphonates	Inhibition	DCPD growth
Carbonate	Inhibition	calcium phosphate nucleation
Cu^{2+}	Inhibition	CP heterogeneous nucleation on DCPD
Sr^{2+}	Inhibition	HAP growth
Sr^{2+}	Inhibition	DCPD growth
Ba	Stabilization	ACP
Pb	Stabilization	ACP
Sn	Inhibition	Calcium phosphate growth
Zn	Increase	OCP growth induction period (>10^{-5}M)

Table 2-3 gives a resume of the effects of various ions on phosphate crystallization and Table 2-4 summarizes the processes occurring in the calcium phosphate system on which Mg has no affect.

Table 2-4. Processes in the calcium phosphate system not inhibited by Mg

Cation	Effect	Process
Mg	No inhibition	ACP1 formation
Mg	No inhibition	ACP1 dissolution
Mg	No inhibition	OCP nucleation
Mg	No inhibition	DCPD growth

2.4 THE ACTUAL CRYSTALLIZATION PROCESS

It has been indicated in Table 2-1 that a large number of solid compounds are important in phosphate removal. Since the current study concentrated on crystallization of HAP, only the happenings in HAP formation and transformation will be discussed in this section.

2.4.1 HAP formation and transformation

HAP is the thermodynamically most stable solid and van Kemenade & de Bruyn (1987) found that the formation of HAP was always preceded by one or more precursors in a sequence that was in agreement with the Ostwald rule of stages. Homogeneous formation of HAP at low concentrations was never observed. The heterogeneous formation of HAP on OCP surfaces was noted to decrease with increasing initial supersaturation.

Calcium phosphates were precipitated at 25°C from solutions of medium and low concentrations in the presence of Mg (Abbona *et al.*, 1992). The solids occurring one year later are brushite in the more concentrated solutions, HAP [$Ca_5OH(PO_4)_3$] and $Ca_9MgH(PO_4)_7$ in the others but it is clear that the transformation can take days to months to form.

The precipitation of HAP from dilute solutions was studied by Boskey & Posner (1976). At comparatively low supersaturations (SI of 10^5 to 10^9), HAP precipitates without the formation of the amorphous calcium phosphate precursor, which was previously believed obligatory. After initial formation the crystals grow by a ripening process with little or no further nucleation.

In solutions of low calcium phosphate concentration, supersaturated only with respect to the thermodynamically most stable HAP, macroscopic amounts of this solid could be grown on HAP seed material without the formation of a precursor phase (Koutsoukos *et al.* 1980)

The kinetics of growth of HAP has been studied (25° C; constant physiological pH) by seeding stable supersaturated calcium phosphate solutions with HAP crystals (Nancollas & Mohan, 1970). During the first 60 to 90 minutes, growth proceeds through the formation of a precursor phase which has a Ca:P ratio of 1,45 ± 0,05. The precursor phase undergoes slow interaction with the medium to transform into HAP. The initial rates of growth are independent of the rate of stirring and are dependent on the seed concentration and supersaturation. This pointed to a surface controlled crystallization reaction (Nancollas, 1971).

The direct precipitation of HAP, from solutions supersaturated only with respect to this solid was studied (37° C; pH 5,0-6,5) under conditions of constant total molar concentrations of Ca^{2+} (1,3-28,9 mM) and phosphate (0,8-8,0 mM), and ionic strength (13,55-109,20mM) (Nancollas & Koutsoukos, 1980). The rate of crystallization of HAP on HAP seed crystals was constant as a function of time. It was not affected by secondary nucleation or stirring. The rate was also linearly dependent on the supersaturation, and the crystallization had an apparent activation energy of 85,5 kJ/Mole. The rate constant for crystallization depends on this number.

Inskeep & Silvertooth (1988) studied the kinetics of HAP precipitation, with [Ca] = 0,38-0,86 mM and [PO_4] = 0,29-1,00 mM; ionic strengths of 0,015-0,043 M and HAP seed concentrations of 7,1-28,4 m^2/ℓ (10-40°C; pH 7,4-8,4). The following empirical rate equation was deduced:

$$R = k_f.S.\gamma_2.\gamma_3[Ca^{2+}][PO_4^{3-}][Mole/\ell s]$$

where k_f = rate constant = 173 ± 11 $\ell^2 mol.m^2.s$; γ_2, γ_3 = divalent and trivalent ion activity coefficients and S = surface area (m^2/ℓ).

The rate law incorporates a term for the surface area, which is further evidence for the hypothesis that the reaction is surface controlled as indicated by the Arrhenius activation energy which was 186 kJ/Mole. Rate-limiting steps in the mechanism include migration of surface Ca^{2+} and HPO_4^{2-} into holes in the lattice, with subsequent dehydration and incorporation into the crystal lattice.

This agreed with the results of Brown & Chow (1981), who studied the rates of dissolution and crystal growth of HAP. They found that the composition of the quasi-saturated solution immediately adjacent to the crystal surface is important in controlling the rate of crystal growth. The composition of this solution shifts, depending on the relative rates of diffusion of Ca^{2+} and PO_4^{3-}. Steady state is achieved when the Ca:P rate-of-diffusion ratio reaches 5:3, the stoichiometric ratios of Ca^{2+} and PO_4^{3-} in the crystalline solid.

It is a reasonable assumption that the same species might exist on the surface of HAP during the crystallization and dissolution processes. In their studies on the dissolution of HAP, La Mer (1962) concluded that HAP undergoes hydrolysis in aqueous solution, to yield a solid surface complex, $Ca_2(HPO_4)(OH)_2$. It is this surface complex, and not HAP, which dominates the solubility equilibrium. These findings are in agreement with those of Deitz *et al.* (1964). Thus it seems that the formation of HAP on HAP seeds involves migration of Ca^{2+} and HPO_4^{2-} ions to the surface of the crystal, followed by adsorption of the ions, formation of a surface complex, and incorporation into the crystal lattice with accompanying dehydration. The incorporation of the ions could be preceded by a surface reaction to give the species that comprises the bulk of the crystal.

2.4.2 Interfering ions

This section contains information of a more general nature on the effects of interfering ions. Various other sections can also be consulted, e.g. see the sub-sections 2.3.6 and 2.4.4.7 on interfering ions in the sections on Thermodynamics and Kinetics respectively.

2.4.2.1 Magnesium

Jenkins *et al.* (1972) found that the presence of Mg reduces crystalline calcium phosphate precipitation at pH < 9. Mg was thought to be acting through disruption of the calcium phosphate crystal lattice, or by adsorbing onto the growing calcium phosphate crystals. A Mg concentration of 1,0 mM is the maximum that can be tolerated before crystalline calcium phosphate precipitation is seriously affected. When

ACP precipitates, Mg seems to have a positive effect, supposedly due to the formation of a magnesium phosphate compound that co-precipitates.

Ferguson & McCarty (1971) studied the effects of moderate amounts of Mg on phosphate removal from solution as a function of pH. At pH below 9, increase of Mg up to 3 mM decreased the formation of calcium phosphate precipitate. At pH values between 9 and 11 increased phosphate removal was obtained upon increased Mg concentration, and little effect on calcium phosphate precipitation was observed above pH 11,5. Solution concentrations of Mg were nearly constant below pH 10, and decreased rapidly at higher pH values.

Experimental results in the $Ca\text{-}CO_3\text{-}PO_4$ system show that magnesium slows the rate of phosphate precipitation at pH 8 (Ferguson *et al.* 1970). In the presence of magnesium at pH 9,5 phosphate residuals increase rapidly from an initial low value to a value dependent on the Mg concentration and increasing Mg concentrations appear to progressively decrease the phosphate residual attained after 5 h.

The effect of Mg and carbonate on calcium phosphate precipitation was investigated at concentration conditions resembling those in the anaerobic digestion process and at concentration ratios typical of waste waters (Ferguson & McCarty, 1971). Chemically defined systems were allowed to precipitate at constant temperatures (20 to 30°C). The precipitation time was usually 24 hours, but in some tests varied from 1 minute to several weeks. After precipitation, the pH was determined, solids were separated and subjected to X-ray diffraction, and the soluble components were analyzed. With Mg present, the phosphate residual decreased gradually; low values were found at pH above 9. Without Mg local minima and maxima in the residual phosphate were found, respectively, at pH 8 and 9,5. Higher carbonate concentrations increased the phosphate residual at pH 8-11. This effect was reduced in systems with high Mg concentrations.

Aqueous solution aragonite-calcite transformation kinetics were studied (Bischoff & Fyfe 1968). The reaction involved solution and equilibration of aragonite with solution, with subsequent nucleation and growth of calcite. Calcite seems to nucleate on the aragonite surface but growth is along point or line defects. CO_2 and $CaCl_2$ catalysis and KOH inhibition indicate a fundamental Ca^{2+} - HCO_3^- reaction and calcite crystallization is strongly inhibited by Mg^{2+} and less so by SO_4^{2-}.

2.4.2.2 Carbonate

Carbonate causes increased phosphate residuals between pH 9 to 10,5 because of competitive $CaCO_3$ precipitation (Ferguson *et al.* 1970). Increasing carbonate concentrations slow the rate of phosphate precipitation and increase the long-term phosphate residual.

III. LABORATORY STUDIES

3.1 INTRODUCTION

3.1.1 Chemical modelling studies

The main objective of the crystallizer is to remove phosphate from the anaerobic effluent at elevated pH between 9,8-10,6 by addition of lime. The lime simultaneously supplements the calcium to a ratio of 2:1::Ca:P which is favourable for the formation of calcium phosphate crystals. However, problems were experienced in the operation of the crystallizer, since $CaCO_3$ crystallizes onto the sand of the fluidized bed in preference to hydroxyapatite. The major problem was the formation of flocs which appeared in the effluent. This problem can occur if the total carbonate concentration of the influent is too high, resulting in the complexation with the calcium from the lime. This then decreases the amount of calcium available to complex with the phosphate, and hence leads to inefficient phosphate removal.

The aim of this study was to establish the effect of varying total carbonate and sulphate ion concentrations in the calcium phosphate crystallization process by using a chemical equilibrium model, JESS, to guide further research on the phosphate crystallization.

The total carbonate concentration of the influent can be markedly decreased if degasssification is applied as a pretreatment step. Efficient removal of CO_2 appears to be possible by acidification with H_2SO_4 before the degassifier. Thus two parameters would be altered with degassification, viz. sulphate ion and total carbonate concentrations. By chemical simulation, JESS attempts to predict how variations of these two parameters will affect the chemical equilibrium of the system and in particular, how it affects phosphate crystallization.

This information was used to determine the viability of degassification, without first having to go to the expense of installing the degassifier to measure its effectiveness.

3.1.1.1 Effect of carbonate concentration on phosphate removal

The composition of the solution used as model is listed below. The concentrations were based on analysis of the particular sample in question, and where elements were not analyzed for, their concentrations were derived from averages of analyses performed over a period of two months.

CO_3	5,412 mM
PO_4	0,807 mM
SO_4	0,958 mM
NH_3	1,100 mM
Ca	0,873 mM
Mg	0,823 mM
Al	0,008 mM
Initial pH:	8
Final pH:	10

A solution containing calcium and phosphate can form solids which contain varying amounts of calcium and phosphate. These include the following:

HAP	hydroxyapatite	$Ca_5(PO_3)_3OH$
TCP	tricalcium phosphate	$Ca_3(PO_4)_2$
OCP	octacalcium phosphate	$Ca_8(HPO_4)_2(PO_4)_4.6H_2O$
Brushite	calcium phosphate dihydrate	$CaHPO_4.2H_2O$

The above four solids are presented in order of decreasing stability when the pH is greater than 7, i.e. HAP is the preferred (most stable) form, and brushite the least preferred form.

A preliminary simulation of the solution was performed, in which the pH of the solution was raised from 8 to 10 by the addition of lime [$Ca(OH)_2$]. The concentration of calcium in the solution as a result of neutralization with lime was high enough to precipitate HAP, TCP and OCP, i.e. at the calcium and phosphate concentrations calculated, all three above solids were supersaturated, and brushite was undersaturated. Calcite (calcium carbonate) was also supersaturated.

The following sections deal with modelling of the precipitation of the above solids.

3.1.1.1.1 Precipitation of hydroxyapatite (HAP) [$Ca_5(OH)(PO_4)_3$]

Initially, the precipitation of HAP was modelled, since it is the most stable phosphate-containing solid that could possibly be formed in the system. The carbonate concentration was scanned over the range 0,05412 mM to 5,412 mM. Phosphate removal was found to be insensitive to carbonate concentration. It was found that even if calcium carbonate precipitated as calcite, there was total removal of phosphate as HAP.

The observation that phosphate removal is affected by carbonate concentration implies that the precipitation reactions are under kinetic control. Under the reigning conditions of the phosphate crystallization, therefore, the formation of HAP is slow, allowing precipitation of a less stable phosphate-containing substance. It has been shown that an empirical generalization, known as the Ostwald-Lussac rule, applies to this system (Ostwald, 1897 cited by Wade *et al.*, 1993). This rule states that, when a number of solids (such as the above) are highly supersaturated, the least stable solid will precipitate first. This condition is in direct conflict with the thermodynamic driving force

to achieve the most stable arrangement. However, once formed, these less stable solids gradually convert to the more stable forms, and ultimately to the most stable crystal.

The higher the supersaturation levels, the more applicable is the Ostwald-Lussac rule, i.e. the more supersaturated the solution, the more likely the less stable forms will occur. Also, the more supersaturated the solution, the greater the potential for homogeneous nucleation, which is the spontaneous formation of crystals which are often internally quite disordered, due to the rate at which they form. Conversely, at low supersaturation, heterogeneous nucleation is favoured, which occurs in a more reproducible way, and in which the crystals formed are much more ordered. Heterogeneous nucleation normally takes place on available surfaces (e.g. suspended sand particles). The crystals tend to be large and fairly robust, thus unlikely to disintegrate, and to be a source of suspended solids. Homogeneous nucleation can result in microcrystals being formed remaining in suspension. Due to the high rate of formation of the crystals, they can be quite fragile, and thus more easily eroded to produce suspended solid particles.

Therefore, further simulations were performed, assuming that OCP or TCP are removed from solution.

3.1.1.1.2 Precipitation of Octacalcium Phosphate (OCP) [$Ca_8(HPO_4)_2(PO_4)_4.6H_2O$]

Following the Ostwald-Lussac rule, as outlined above, simulations were performed on the test solution, assuming that the least stable calcium phosphate solid, OCP, precipitated.

The phosphate removal was found to be relatively insensitive to carbonate concentration below the solubility of calcite (calcium carbonate), and was constant at a removal value of 97,6 %.

However, when there was enough carbonate to precipitate the calcite, the phosphate removal decreased to zero. Phosphate removal remained at this level as carbonate concentration was increased above the level required to precipitate calcite.

3.1.1.1.3 Precipitation of tricalcium phosphate (TCP) [$Ca_3(PO_4)_2$]

In the absence of information pertaining to the relative rates of precipitation of the calcium phosphate solids, it is possible that OCP forms quickly, then transforms to the next least stable possible calcium phosphate solid, TCP, fairly rapidly in the time frame of the crystallization process. Simulations were performed on the test solution, assuming that TCP precipitated. The results obtained were similar to that of the model of precipitation of OCP.

The phosphate removal was found to be relatively insensitive to carbonate concentration below the solubility of calcite (calcium carbonate), and was constant at a removal value of 99,4 %.

When there was enough carbonate to precipitate the calcite, the phosphate removal

decreased to 0,0%. Phosphate removal remained at this level as carbonate concentration was increased above the level required to precipitate calcite.

In practice, however, the amount of phosphate actually removed depends on the relative rates of precipitation of calcite and the phosphate-containing solids.

Thus the system is under kinetic control, but the thermodynamic boundaries are clearly defined - low carbonate leads to high removal of phosphate as OCP or as TCP, and high carbonate leads to low removal of phosphate as OCP or as TCP.

Therefore, it is desirable to remove carbonate. One method of removal entails acidification with H_2SO_4 to pH 4, removal of carbonate as CO_2, and restoration of the pH with $Ca(OH)_2$. The effect of the added sulphate is modelled in section 3.1.1.2 below.

3.1.1.2 Effect of sulphate concentration on phosphate removal

A titration of the solution in section 3.1.1.1 to a pH of 4,0 was simulated, to establish the amount of sulphuric acid needed, and therefore the amount of sulphate added to the system. The sulphate resulting from this process was computed to be 0,001862 moles/litre.

The pH was then increased to 10,0 by the addition of $Ca(OH)_2$, and the solubility of gypsum (calcium sulphate) was calculated.

The log SI of gypsum was calculated to be -1.6, implying that gypsum is undersaturated at these conditions, and therefore will not precipitate. It also means that more sulphate may be added to the system before the sulphate removes calcium appreciably, and hinders phosphate removal as calcium salts. Therefore it is feasible to remove carbonate by an acidification process.

3.1.1.3 Summary of chemical modelling

The precipitation of calcium phosphate species in the crystallizer is largely under kinetic control, and the most stable possible solid, HAP, is not precipitating first.

Regardless of whether the solid precipitating first is TCP or OCP, the system is sensitive to carbonate (or bicarbonate) concentration of the order of that required to precipitate calcium carbonate as calcite. Low carbonate leads to high removal of phosphate as OCP or as TCP, and high carbonate leads to low removal of phosphate as OCP or as TCP. Therefore it is desirable to remove carbonate for adequate phosphate removal by precipitation.

The amount of sulphate, derived from sulphuric acid, required to acidify the system to a pH of 4, prior to blowing off of carbon dioxide, is substantially lower than the concentration of sulphate which would interfere with phosphate removal by crystallization. Therefore it is feasible to remove carbonate by an acidification process.

3.2 MATERIALS AND METHODS

Based on the results of the chemical modelling, laboratory scale evaluations were conducted as described in the following sections.

3.2.1 Chemical analyses

Standard methods (1989) were used for analyses of total and ortho-phosphate, as well as for determination of calcium and pH.

3.2.2 Experimental system

Laboratory reactors with lengths of ca. 1 m and internal diameters of 40 mm were used. The configuration of the laboratory system (Momberg, 1993a) was adapted such that the recycle ratio could be altered from ca. 0,5 to 25. Settled supernatant was degassed through adjustment of pH to 4,0-4,5 using sulphuric acid, and aeration to remove CO_2. The degassed influent was fed to the laboratory crystallizer at the base of the reactor.

In order to understand the underlying principles and interactions of the various mass transfer phenomena taking place in the crystallizer, phosphate precipitation, i.e. crystallization and flocculation, were quantified by means of the following simplified steady state mass balance over the reactor:

Total o-phosphate in = Total o-phosphate out

Total o-phosphate in = $UF(o\text{-}P)_f$

= $F(o\text{-}P)_f + d(o\text{-}P)_f$

Total o-phosphate out = $UF(o\text{-}P)_e + X(o\text{-}P)$

= $F(o\text{-}P)_e + Z(o\text{-}P)_e + d(o\text{-}P)_f + X(o\text{-}P)$

Where
- o-P : ortho-phosphate
- UF : total of unfiltered sample
- F : soluble part of filtered sample
- d = UF-F : insoluble part filtered out
- X : crystals
- Z : amorphous flocs, in suspension
- subscript f : feed influent to reactor
- subscript e : effluent out of reactor.

From this follows that:

$d(o\text{-}P)_f$ = $UF(o\text{-}P)_f - F(o\text{-}P)_f$

= insoluble part of the feed not susceptible to precipitation, and will flow through the fluidized bed.

$d(o\text{-}P)_e$ = $UF(o\text{-}P)_e - F(o\text{-}P)_e = Z(o\text{-}P)_e + d(o\text{-}P)_f$

= insoluble part of the effluent consists of flocs formed plus the insoluble part of the feed influent.

The primary objective with the crystallizer is to have as little as possible ortho-phosphate in the effluent leaving the crystallizer. This is achieved by precipitating as much of the o-phosphate in solution in such a way that the biggest fraction of the reacted o-phosphate is retained in the crystalline form, as contrasted to the remaining part that will be carried over as amorphous flocs in suspension.

To compare the influences that the different parameters have on the crystallization, it is however not sufficient to simply look at the filtered and unfiltered values of the effluent; for example the higher the pH the more ortho-phosphate precipitates, although more crystals are formed more flocs are then also carried over.

Crystallization efficiency (%X) is an important parameter to establish the effectivity of the process. It is defined as that fraction of the ortho-phosphate precipitated that has formed crystals and not amorphous flocs and has been used in the presentation of the results. Using the mass balance this can easily be calculated with the ortho-phosphate values of the filtered and unfiltered samples of the feed and effluent:

$$\%X = \frac{X(o\text{-}P)}{X(o\text{-}P) + d(o\text{-}P)_e}$$

$$= \frac{UF(o\text{-}P)_f - UF(o\text{-}P)_e}{F(o\text{-}P)_f - F(o\text{-}P)_e}$$

3.3 DISCUSSION OF RESULTS

The major aim of the crystallization process is to achieve maximum crystal formation with a minimum of floc formation. The flocs are washed out of the column and the phosphate is not recovered on the sand bed acting as crystallization nuclei. Laboratory experiments were therefore conducted to establish the desired conditions for the evaluation of the pilot-scale process.

3.3.1 Influence of recycle ratio

The *recycle ratio* (R) is defined as the recycled flow rate divided by the influent flow rate. The total flow rate through the crystallizer is kept reasonably constant to maintain a linear velocity of 40 - 80 m/h. The reason for this is to ensure proper fluidization and at the same time satisfy the reaction kinetics, i.e. to allow sufficient time for precipitation to take place in a properly fluidized bed.

An increase in the recycled flow rate would imply a corresponding decrease in the influent flow rate, with a consequent increase in the retention time. Increasing the recycle ratio would further also have the effect of diluting the o-phosphate concentration entering the reactor. The recycle ratio can thus be expected to have a significant influence on the performance of the crystallizer.

The influence of recycling on the overall reduction in soluble o-phosphate (filtered samples) is illustrated by the laboratory results represented in Fig. 3-1. As expected,

the results generally showed that at higher recycle ratios less o-phosphate remained in solution at any specific pH. This trend was again reflected in Fig. 3-2 which indicated that at higher recycle ratios more crystals were produced. Fig. 3-3 depicts the influence of recycling on the overall crystallization effectivity. It can be seen that the lower the recycle ratio the less efficient the crystallization became, i.e. the percentage of flocs was increased. This effect appeared to be especially pronounced at low recycle ratios.

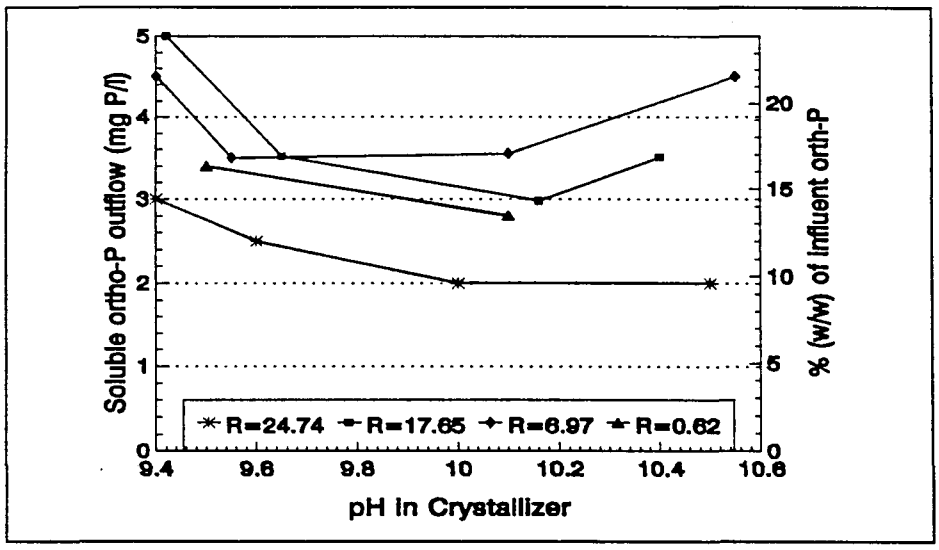

Fig. 3-1. **The influence of recycling on the overall reduction in soluble o-phosphate**

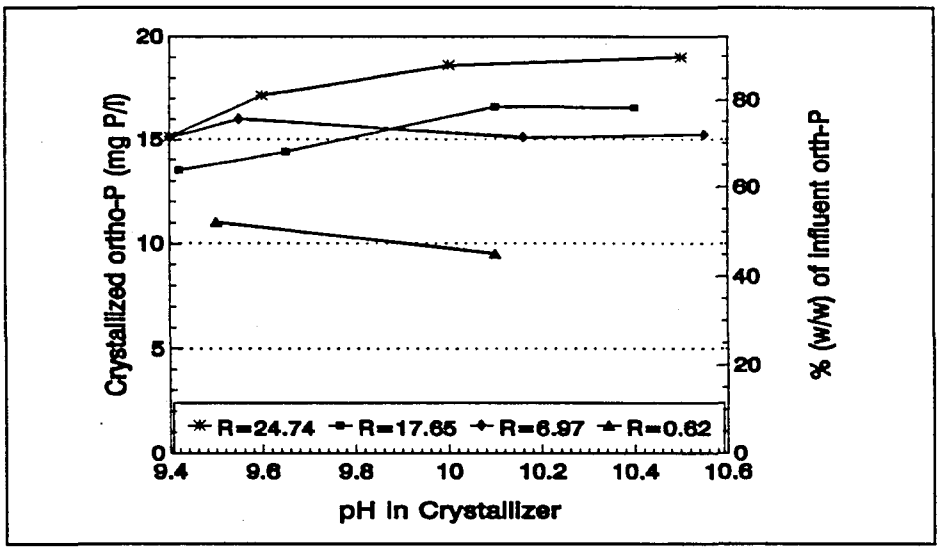

Fig. 3-2. **The influence of recycling on the formation of crystals from o-phosphate**

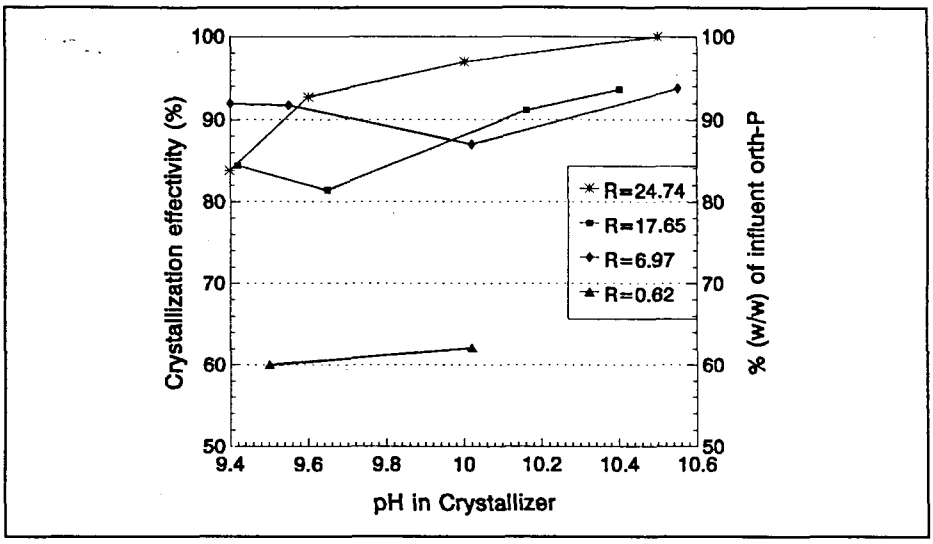

Fig. 3-3. The influence of recycling on the o-phosphate crystallization effe ctivity

The laboratory system was limited in its adaptability to conduct experiments accurately at low recycle ratios. To establish the desired recycle ratio, therefore, for full-scale application, the data from Fig. 3-2 on the amount of crystallization was plotted against the recycle ratios at pH 10. The data are presented in Fig. 3-4. It was evident that the recycle ratio exerted its main effect at ratios up to R = 7. A further increase in recycle ratio up to R = 24,74 had a limited adavantage. Eggers *et al.* (1991a) used a recycle ratio of 1. However, the phosphate concentration in the effluent treated was approximately 5 mg/ℓ compared to more than 20 mg/ℓ in the current investigation. The difference in the phosphate concentrations could affect the crystallization efficiency.

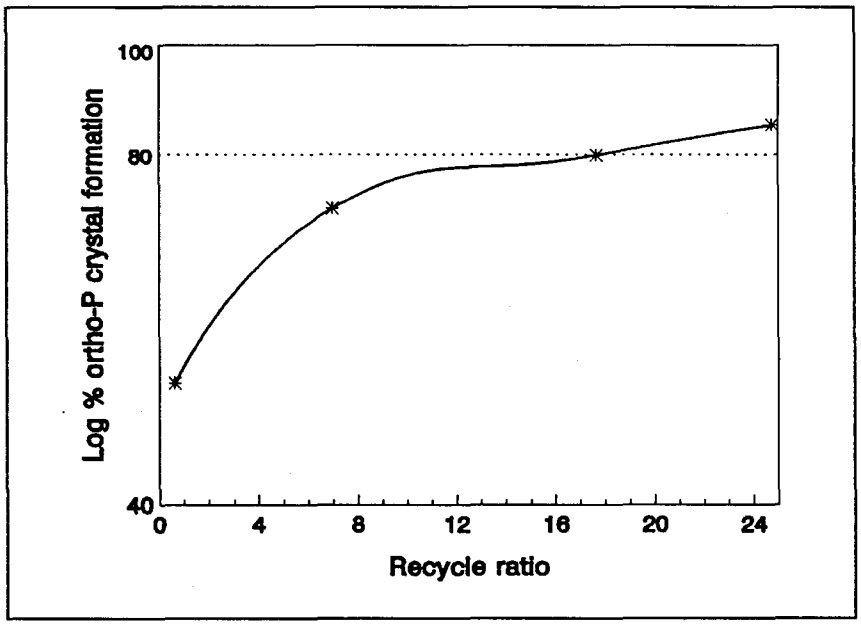

Fig. 3-4. The influence of recycle ratio on crystallization

3.3.2 Optimum crystallization pH

Extensive laboratory investigations (Momberg, 1993a) showed that the pH for HAP removal should be above pH 9. A very high pH would cause supersaturation to occur with the resultant undesirable formation of flocs, whereas a pH that is too low would result in a slow crystal growth.

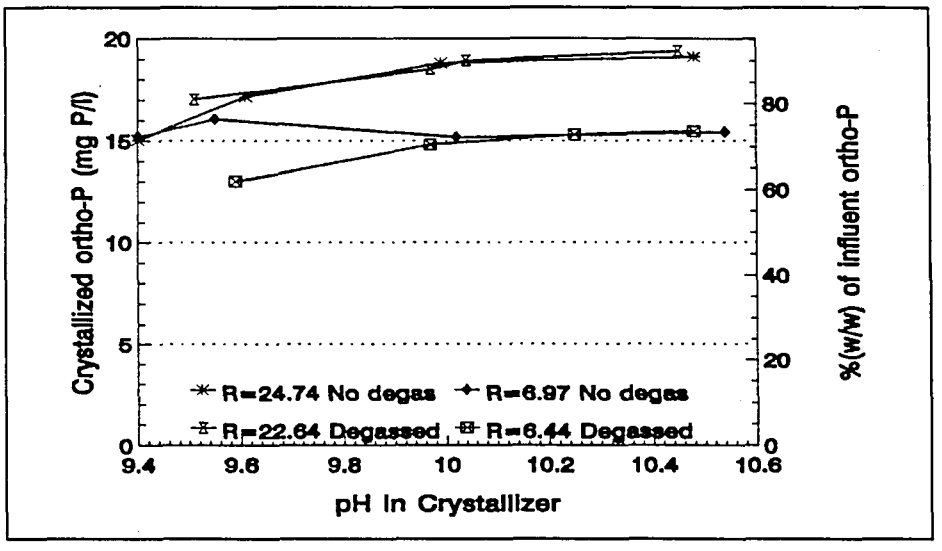

Fig. 3-5. **The influence of degassing on the formation of crystals from o-phosphate**

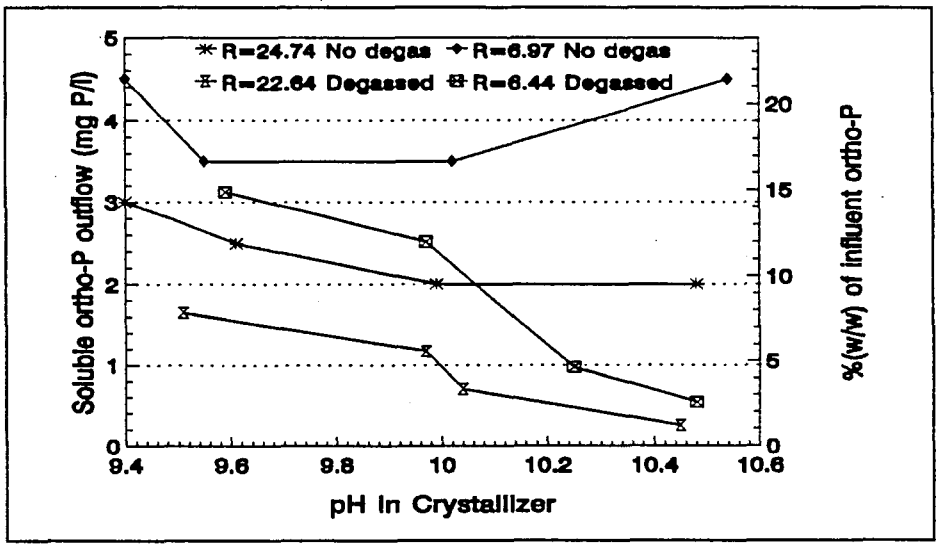

Fig. 3-6. **The influence of degassing on the overall reduction in soluble o-phosphate**

3.3.3 Effect of degassing

The presence of dissolved carbon dioxide, in the form of carbonate and bicarbonate, in the influent can affect the crystallization in several ways. At a high pH calcium carbonate will precipitate out of solution, thus reducing the calcium available for crystallization of HAP. Furthermore, the inclusion of carbonate has a weakening effect on the mechanical properties of the crystals (Eggers *et al.*, 1991b). In the process of $CaCO_3$ precipitation, additional seed material is formed. However, this has a detrimental effect as HAP crystallizing out onto the very light $CaCO_3$ seed is washed out of the column. Phosphate removal efficiency is in this way reduced.

The experimental results presented in Fig. 3-5 indicate that degassing did not have a significant influence on the amount of o-phosphate crystallized. However, Fig. 3-6 shows that after degassing there was a decrease in the o-phosphate remaining in solution. It would thus appear that the amount of crystals formed is the same for both types of influent, and that the additional phosphate removed in the degassed influent is in the form of amorphous flocs. A possible explanation for this lies in the differing concentrations of carbonate anions. Degassing serves to decrease the concentration of carbonate ions in the influent. However, carbonate ions have a buffering action, which would be very much decreased in the degassed influent. One would expect, therefore, that the optimal pH range when using degassed feed is of greater importance and lies in a smaller range, than when a buffering effect is present. Should efficient mixing not occur, this would result in areas of supersaturation caused by too high a pH. The positive effect of degassing would thus not be evident, i.e. the extra phosphate that is removed will be evident as flocs, rather than as crystals.

It therefore appears that degassing does have a positive effect, which is supported by experimental results of decreased soluble o-phosphate in the outflow. The reason why crystallization effectivity is not increased is due to inefficient mixing. Once correct mixing has been achieved, the advantages of degassing should become evident in less soluble o-phosphate in the outflow and a higher crystallization effectivity.

A further apparent anomaly appears in Fig. 3-6 where the concentration of o-phosphate increases with increasing pH under certain operating conditions, with the influent that has not been degassed. Without degassing, the influent has both carbonate and ortho-phosphate ions present. At a high pH, both $CaCO_3$ and HAP would precipitate and would be competing for calcium ions.

3.4 CONCLUSIONS

The laboratory system used had its limitations and it was difficult to adjust recycle ratios accurately at low flows. This resulted in a lack of data between minimum fluidization, which was achieved at R = 0,62, and the following data point at R = 6,97. However, the semi-logarithmic plot of recycle ratio against the percentage of ortho-phosphate crystal formation (Fig. 3-4) illustrates that the main effect of recycling was observed between minimum fluidization and R = 7. More work would therefore be necessary to accurately establish the optimum recycle ratio.

These observations were explained by the fact that an increase in the recycle ratio increased the retention time and diluted the influent o-phosphate concentration, with a resultant positive influence on the crystallization effectivity. At low recycle ratios of the order of 1 the crystallization effectivity of the laboratory crystallizer was found to be as low as 62% at a pH of 10 and 32% of the o-phosphate precipitated as amorphous flocs that were carried over.

The recycle ratio should, however, not be greater than 7 as it appears (Fig. 3-6) that $CaCO_3$ precipitates preferentially at a recycle ratio of about 7 and at a pH greater than 10, thus increasing the concentration of o-phosphate in the outflow. With the degassed influent, the carbonate concentration is much reduced, hence phosphate is preferentially removed from the solution at all pH values. As expected, the concentration of o-phosphate in the outflow continues to decrease with increasing pH. This effect is not as noticeable at high recycle ratios where the reactor configuration is closer to a completely mixed, rather than to a plug flow system. Thus, degassing should have a favourable effect once efficient mixing has been established.

The close interrelationships which exist between the different factors of importance for effective crystallization indicate the significance of accurate operational control to achieve success in the application of the technology.

IV. PILOT PLANT STUDIES

4.1 INTRODUCTION

The Crystalactor® was developed and patented by DHV Consultants, of the Netherlands, on the basis of more than 20 years experience with pellet reactors for softening of drinking water, with strong support of the Dutch Government, water authorities and the industry. Research on phosphate crystallization started in the late 1970's and through the mid 1980's the process was developed to pilot and semi-technical scale. The main characteristic of the process is the crystallization of calcium phosphate in a granular form in a fluidized bed reactor. In 1988 the first full-scale (200 m^3/h) reactor was put into operation at Westerbork, the Netherlands (Eggers *et al.*, 1991a,b.)

The purpose of developing and operating the pilot plant crystallizer was essentially to establish the feasibility of scaling up the crystallization process for full-scale application, and to determine the influence on the other stages of the water treatment process.

The design and development of the pilot plant crystallizer in this study was based on the experience gained with the laboratory scale model, the somewhat sparse and generalized literature on pilot and full-scale phosphate crystallizers, and fluidization and crystallization theory. As will become evident, scaling up from the laboratory to the pilot plant posed a number of unforseen practical problems of the process on a larger scale.

4.2 PROCESS DESCRIPTION

4.2.1 Pilot plant location and integration

The pilot plant was located at module nine of the three-stage modified Bardenpho process of the Daspoort Water Care Works of the City Council of Pretoria.

In brief, the Bardenpho water treatment process utilizes three distinct reactor basins: anaerobic, anoxic and aerobic zones, which are linked by feed and recycle streams. Phosphates are absorbed by the microbial biomass in the aerobic zone, and after recycling of the biomass to the anaerobic zone, the phosphates are released into the supernatant of the anaerobic zone. Typically phosphates of less than 10 mg P/ℓ in the influent are thus concentrated to values greater than 50 mg P/ℓ at the end of the anaerobic phase. Consequently, for optimum phosphate removal the phosphate crystallizer pilot plant was integrated with the anaerobic phase of the process. A submersible pump supplied the settling tank with mixed liquor from the end of the anaerobic phase, the settled sludge and crystallizer effluent was returned to the beginning of the anaerobic zone.

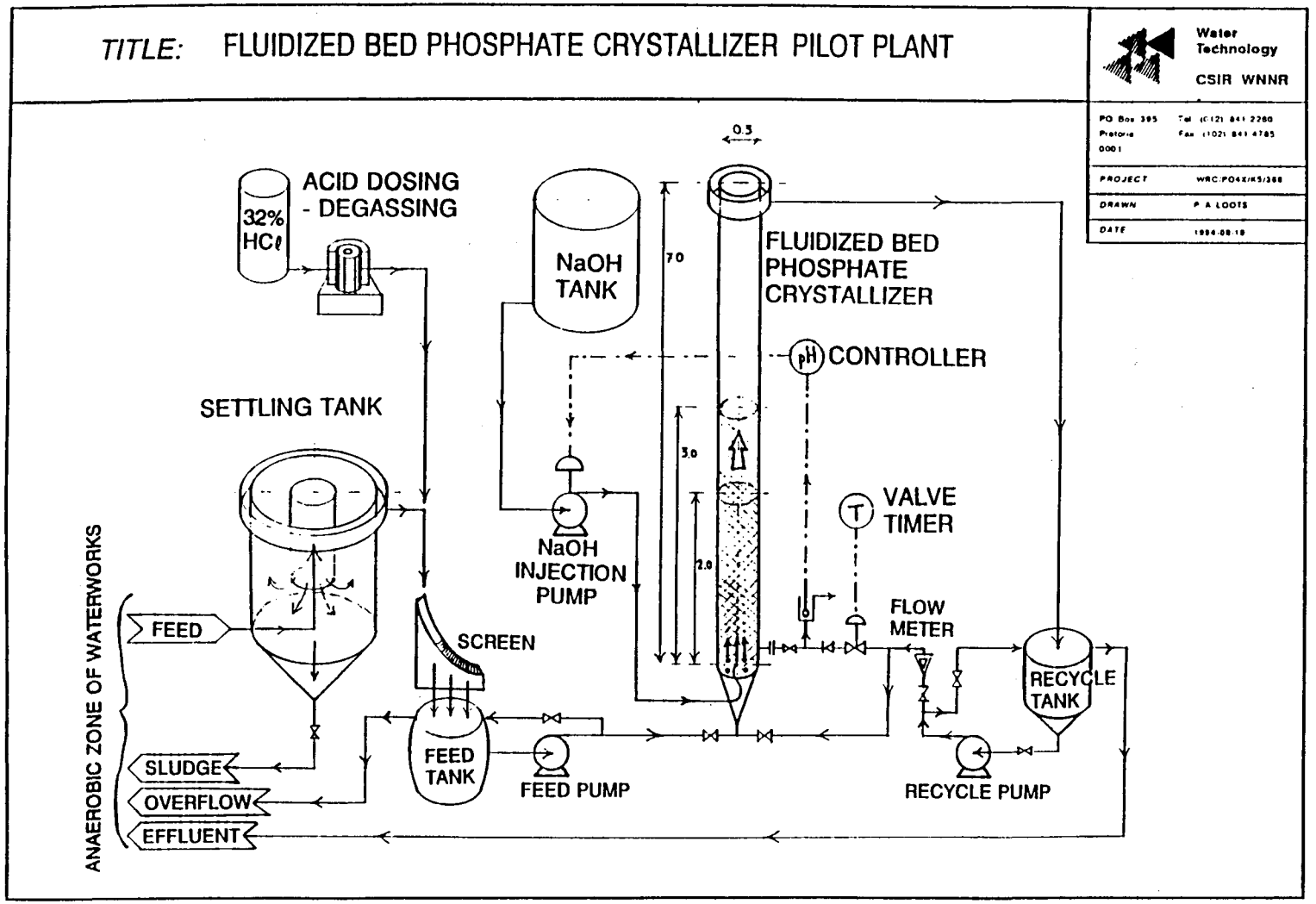

Fig. 4-1. Flow diagram of the fluidized bed phosphate crystallizer pilot plant

4.2.2 Pilot plant layout

Fig. 4-1 presents a detailed flow diagram of the pilot plant. The process units are depicted with the most important dimensions, the pipe system with valves indicate the process streams, and the pumps and instrumentation are displayed schematically.

4.2.2.1 Settling tank

A submersible pump at the end of the anaerobic zone pumped 4,5 m^3/h mixed liquor through a 40 mm ID pipe (1,0 m/s) into the 0,6 m stilling column of the settling tank. A 55 % sludge draw off into the beginning of the anaerobic zone produced a settling rate of 0,6 m/s with ca. 1,8 m^3/h supernatant.

4.2.2.2 Crystallizer feed

The supernatant then cascaded down a sloped screen to remove floatable particles that were carried over. The screen was positioned on top of the 1,0 m^3 feed tank wherein the supernatant collected for withdrawal by the level controlled feed pump, which pumped the feed to the crystallizer inlet at ca. 1,8 m^3/h (43 m^3/d) through a 25 mm ID pipe (1,0 m/s).

4.2.2.3 Degassing

During the investigation of the effect of degassing on crystallization, 32 % hydrochloric acid was introduced into the supernatant at the settling tank outlet. The reduced pH converted the carbonate species to free CO_2 which was liberated to the atmosphere when the acidified supernatant cascaded 1,4 m down the sloped screen into the feed tank.

4.2.2.4 Calcium supplementation

Provision was initially made for calcium chloride dosing to the feed to ensure the calcium demand of the crystallization reaction. However, analyses invariably showed an excess of calcium already present in the supernatant, thus making calcium supplementation unnecessary.

4.2.2.5 Recycling

The 3,0 m^3/h crystallizer effluent flowed into the 0,5 m^3 recycle tank, from which the recycle pump returned 1,2 m^3/h through a 25 mm ID pipe to the crystallizer inlet. The combined feed and recycle streams thus made up the 3,0 m^3/h crystallizer influent required for fluidization. The 1,8 m^3/h balance of the crystallizer effluent overflowed from the recycle tank into the beginning of the anaerobic zone of the water treatment works.

4.2.2.6 Fluidized bed crystallizer

The crystallizer comprised a 7,0 m high 0,3 m ID column, standing on a four legged table foundation and supported by cables and a scaffold construction. A 0,5 m high cone below the table constituted the inlet of the feed and recycle streams to the crystallizer column. Bolted between the flanges of the column and inlet cone was the

inlet distributor plate, which distributed the influent to the column to bring about stable fluidization of the 2 m sand column (see *4.3.1 Fluidization and flow rate*). The distributor plate also served the additional function of dispersing the sodium hydroxide injected for pH control during crystallization.

At the influent flow rate of 3,0 m^3/h, the 0,49 m^3 volume of the column resulted in a residence time (HRT $\doteq$ V/Q) of 0,16 h (9,9 minutes), and the linear velocity (u = Q/A) of the water through the column was 42 m/h.

4.2.2.7 pH control system

To raise the pH of the crystallizer influent to the crystallization level 43 kg 100 % sodium hydroxide flakes were dissolved in the 4,1 m^3 capacity tank to give a 1,06 % sodium hydroxide solution. The pH in the column, 0,2 m above the distributor plate, was measured with a glass electrode connected to a programmable logic controller (PLC) which regulated the injection pump to maintain the preset crystallization pH.

4.3 PROCESS PERFORMANCE

The crystallizer was designed with the requirements for optimum process performance in mind and the design criteria used are discussed in *Appendix 1, Pilot plant design.*

4.3.1 Fluidization and flow rate

One of the prerequisites for optimum crystallizer performance was to maintain a liquid flow rate that ensures a stable well fluidized bed. To determine the relationship between fluidization and fluid velocity, the pilot plant was operated at a number of different flow rates while measuring the height of the fluidized bed. The results in Fig. 4-2 show that the 2 m sand bed fluidized to 3 m at a linear fluid velocity of 43 m/h (i.e. a flow rate of 3 m^3/h.)

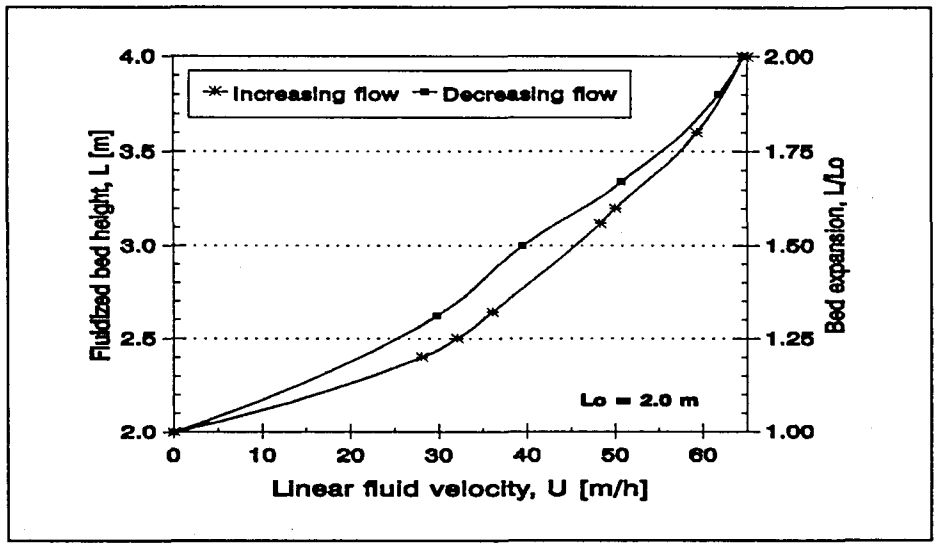

Fig. 4-2. Relationship between the fluidized bed height (L) and the linear fluid velocity (Um)

4.3.2 Non-ideal flow and mixing behaviour

Tracer studies were conducted to ascertain the flow and mixing efficacies at the various flow rates. The sand bed was fluidized at a velocity of 60 m/h with tap water. A calcium chloride tracer pulse was injected into the influent of the crystallizer. The conductivity of the water was monitored both after the inlet distributor and at the crystallizer outlet. Fig. 4-3 shows the response curves at the two measuring points.

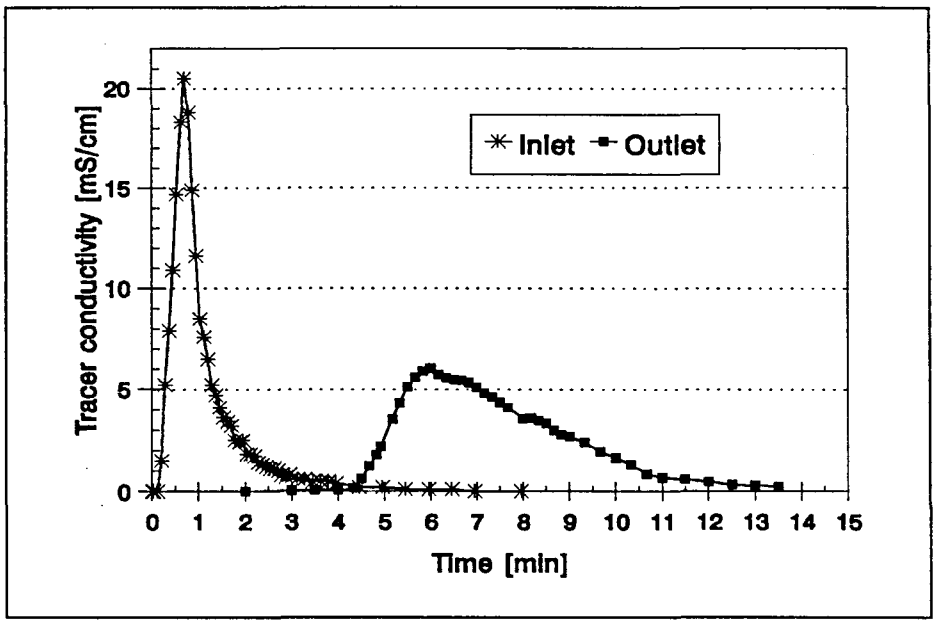

Fig. 4-3. Response curves for a pulse tracer input

4.3.2.1 Inlet mixing analysis

Fig. 4-4 shows the experimental response curve of the crystallizer inlet distributor, compared with the curves of an ideal completely mixed reactor and ideal plug flow reactor.

The mixing behaviour of the inlet system is qualitatively in between those of the two ideal extremes, and consequently a residence-time distribution (RTD) analysis was done to quantify the mixing behaviour of the inlet system.

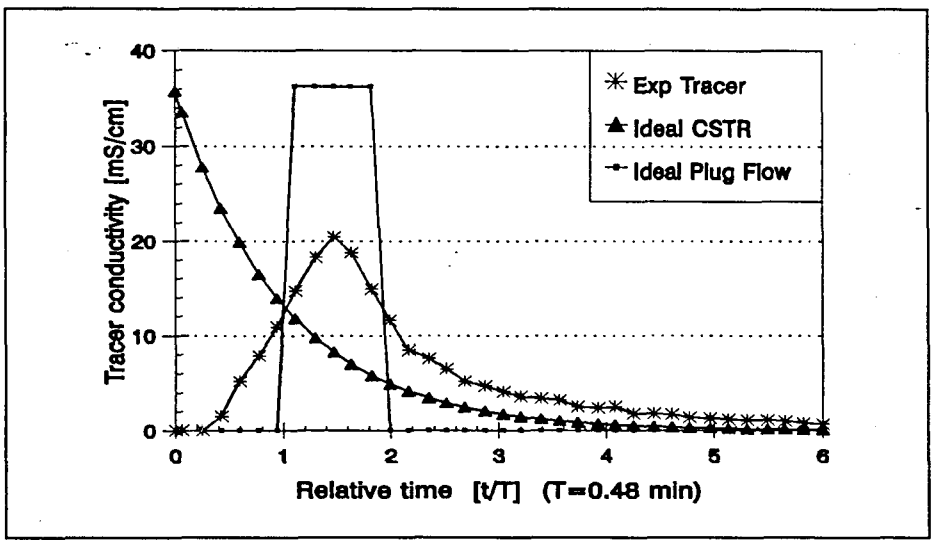

Fig. 4-4. Crystallizer inlet response curves for a pulse tracer input

In Fig. 4-5 the experimental RTD-curve of the inlet system is fitted to the curves of two models of simulated non-ideal flow behaviour. The first half of the inlet mixing behaviour correlates with that of 6 continuously stirred tank reactors (CSTR) in series, while the second half correlates with a plug flow reactor. This may be expressed by the Peclet number (Pe). It is a dimensionless number which indicates axial dispersion (diffusion): Pe = 0 complete mixing, and Pe = ∞ no mixing, i.e. plug flow as discussed in detail by Levenspiel (1972). The inlet system, which has a Pe of 2,9 exhibits moderate and acceptable mixing.

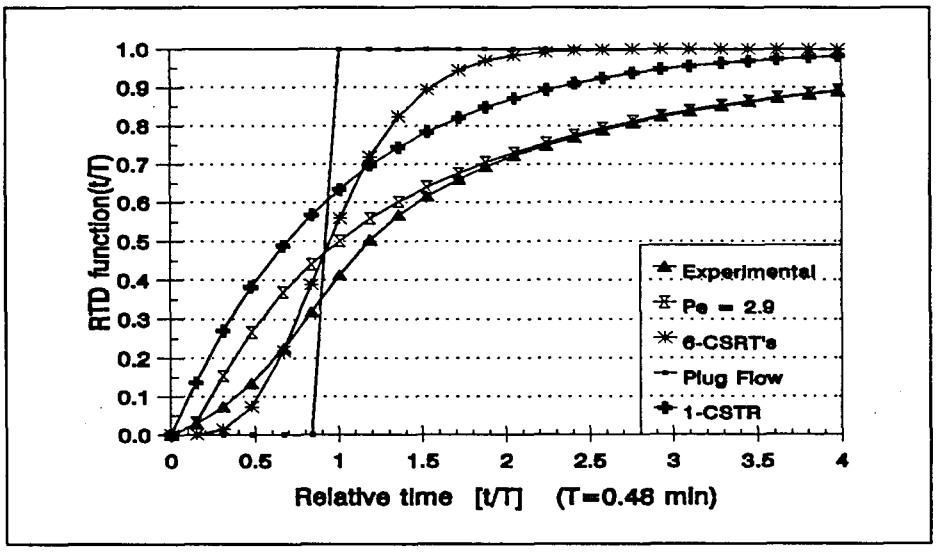

Fig. 4-5. Residence-time distribution of the crystallizer inlet response to a pulse tracer input

4.3.2.2 *Outlet Mixing Analysis*

Fig. 4-6 shows the experimental response curve of the crystallizer outlet, which is the sum effect of the overall mixing behaviour, including that of the inlet system. Again, the overall mixing behaviour is between that of an ideal completely mixed reactor and an ideal plug flow reactor, and a RTD analysis was done to quantify the overall mixing behaviour of the crystallizer.

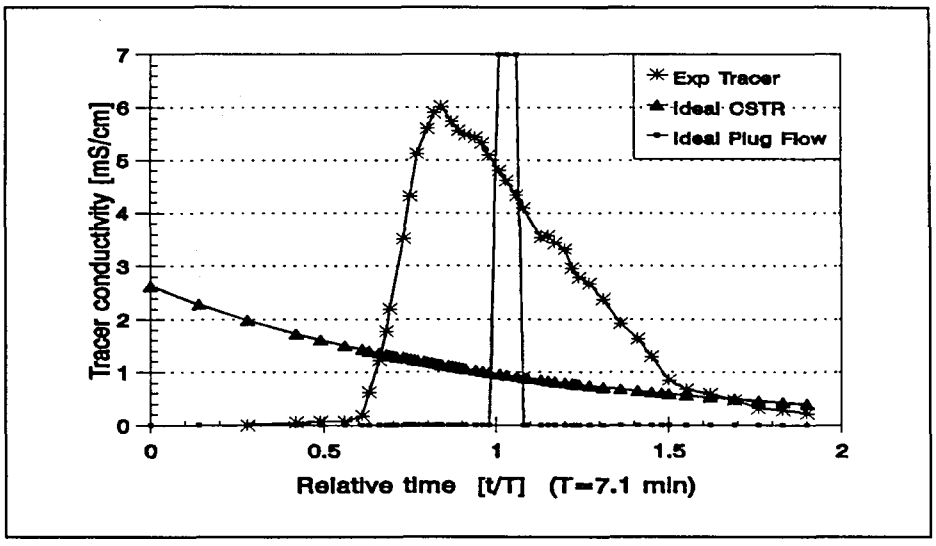

Fig. 4-6. Crystallizer outlet response curves for a pulse tracer input

The RTD analysis of the outlet (Fig. 4-7) correlates the overall mixing behaviour of the crystallizer, including that of the inlet, with a plug flow reactor with little mixing indicated by the Peclet number of 36. The mixing through the inlet system alone was more intense (Pe = 2,9), which consequently means that the mixing behaviour through the rest of the fluidized bed approximates ideal plug flow (Pe > 36). These results are substantiated by similar tracer tests by van Dijk & Wilms (1991) on a full-scale reactor (diameter 2,6 m), which indicated good plug-flow behaviour with a small amount of backmixing (Pe = 100).

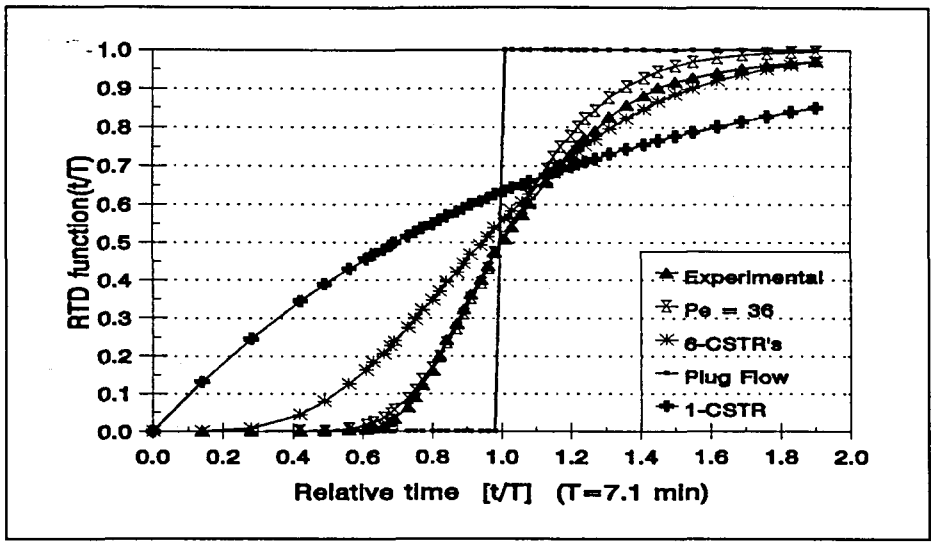

Fig. 4-7. **Residence-time distribution of the crystallizer outlet response to a pulse tracer input**

4.3.3 Recycle ratio

The fluidization and flow rate studies indicated that a minimum linear fluid velocity of 42 m/h (i.e. a flow rate of 3 m^3/h.) is required to achieve fluidization. The settling tank, that supplied the feed tank, delivered a maximum flow rate of 1,8 m^3/h. The remainder of the required water (1,2 m^3/h) was supplied through a recycle of the crystallizer effluent. This indicated a minimum recycle ratio (R) of 0,67 (see Table 4-1); where the recycle ratio is defined as the ratio of flow rate of water recycled, to the flow rate of influent water.

Table 4-1. **Flow rate and recycle ratio combinations**

Feed Q_f [m^3/h]	Recycle Q_r [m^3/h]	Influent Q_t [m^3/h]	Recycle Ratio $R = Q_r/Q_f$
1,8	1,2	3,0	0,67
1,2	1,8	3,0	1,50
0,9	2,1	3,0	2,33
0,6	2,4	3,0	4
0,4	2,6	3,0	7

An increase in recycle ratio has the advantage of diluting the influent concentrations to the reactor, thus stabilizing the process by making the crystallization reaction less intense and enhancing crystallization efficacy. However, the flow rate of the feed stream is inversely proportional to the recycle ratio and a greater recycle ratio implies that less water is treated. The scale of the process also imposes a maximum limit on the flow rate of the recycled stream.

Furthermore, the combination of the feed and recycle streams (i.e. the influent to the reactor) should not contain more of a product (e.g. 'carry-over' flocs) than the process effluent, because this would result in excessive accumulation of the product in the recycle loop. The recycle ratio becomes particularly critical to process performance and demands careful consideration, especially when the recycled product adversely affects the reactor effectivity, as is the case with 'carry-over' flocs in crystallization. For these reasons DHV applies two recycling criteria to their larger scale processes (see Table 4-2, for example):

1. A maximum recycle ratio of R = 1 is used.
2. The crystallizer effluent is passed through dual-media pressure filters for removal of amorphous phosphate particles, before the water is recycled back to the crystallizer.

Table 4-2. Stream data for the full-scale Crystalactor® at Westerbork (Eggers & Kiestra, 1988; Eggers *et al.* 1991a)

Process parameter	Flow rate [m^3/h]	o-Phosphate [mg P/ℓ]
CRYSTALACTOR®		
Feed (downstream of sewage treatment plant)	100	7,5
Recycle 1:1 (from filter effluent)	100	0,5
Influent (Feed + Recycle)	200	4,0
Effluent (Influent to filters)	200	1,7
DUAL-MEDIA PRESSURE FILTERS (Two)		
Effluent (half recycled to Crystalactor®)	200	0,5

These considerations, and the fact that the pilot plant under investigation did not employ filtration of the effluent, indicate that the only reasonable recycle ratio that could be used was the minimum of R = 0,67 needed to achieve fluidization.

4.3.4 Pilot scale degassing

In crystallization the phosphates compete with any carbonates present, according to their precipitation equilibrium constants, for the available calcium and hydroxide ions. Qualitatively, a phosphate of 0,65 mM (20 mg P/ℓ) is overshadowed by a total carbonate of 4 mM (400 mg/ℓ $CaCO_3$) or higher, which has a greater driving force for precipitation. For sufficient phosphate crystallization in the presence of the carbonate, a higher pH and calcium driving force are required, which accordingly further increase the driving force of the carbonate precipitation. This in turn intensifies homogeneous nucleation of the calcium carbonate, resulting in adverse 'carry-over' of precipitated flocs that were not crystallized. Furthermore, an increase in carbonate content causes a weakening in the mechanical strength of the crystals, which aggravates 'carry-over' through abrasion of the crystals. Eggers *et al.* (1991b) demonstrated that a total carbonate ($CT = CO_2 + HCO_3^- + CO_3^{2-}$) value of 2 mM $CaCO_3$ (200 mg/ℓ $CaCO_3$) or less is required to give a mechanically stable pellet with a low carbonate content.

Crystallization studies by Eggers & Kiestra (1988), using an average of 9 mg P/ℓ water, produced pellets with 10 % $CaCO_3$ at a CT of 1-2 mM $CaCO_3$, and pellets with 50% $CaCO_3$ at a CT of 6 mM $CaCO_3$.

In order to investigate the influence of the total carbonate species on the crystallization performance, the carbonates were removed from the water through CO_2 degassing. The carbonate and bicarbonate equilibria were first shifted to the free CO_2 forms, by continuous injection of concentrated 32 % hydrochloric acid into the supernatant at the settling tank outlet. Subsequently, the CO_2 was liberated from the water through cascading 1,4 m into the feed tank. The distribution of the carbonic species in the water after degassing were analyzed for a range of acid flow rates and pH values to verify the degassing effectivity and to determine the acid injection flow rate for optimum degassing, i.e. minimum acid required to achieve a CT of 2 mM $CaCO_3$.

When the total alkalinity of a water is due almost entirely to hydroxides, carbonates, or bicarbonates, and the total dissolved solids is not greater than 500 mg/ℓ, the concentrations of the species can be calculated from the pH and total alkalinity, using the carbonic acid equilibrium constant expressions.

Total alkalinity is generally determined volumetrically by titrating with 0,02 N sulphuric acid to a potentiometric end-point pH, specified for different ranges of alkalinity (Standard Methods, 1989). However, the equivalence points are dependent on the total carbonic species concentration. Therefore, titrating to a predetermined end point may give incorrect results (Benefield *et al.*, 1982), especially where the CT value becomes very small, as in degassing. Thus, to obtain accurate alkalinity measurements, the end points were determined from titration curves, such as illustrated in Fig. 4-8.

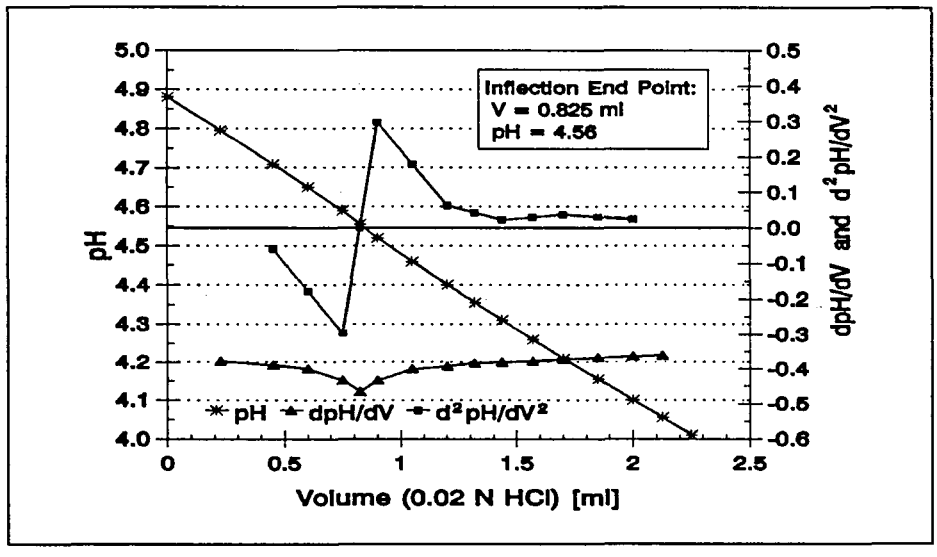

Fig. 4-8. Alkalinity titration curve for water degassed at pH 4,88

Fig. 4-9 shows the distribution of the carbonate species in the water, after cascade degassing, as a function of pH. As the pH is lowered the CO_3^{2-} is systematically converted to HCO_3^-, which in turn is converted to free CO_2 which escapes to the atmosphere during cascade degassing. The total carbonate decreases accordingly from 4 mM $CaCO_3$ at the initial pH of 7,25, to the desired 2 mM $CaCO_3$ at a pH of 4,75. (The influence of degassing on crystallization performance is discussed further in section *4.3.5 Crystallization*, and some practical difficulties experienced with degassing on pilot scale are reviewed in *Appendix 2, Pilot plant operation.*

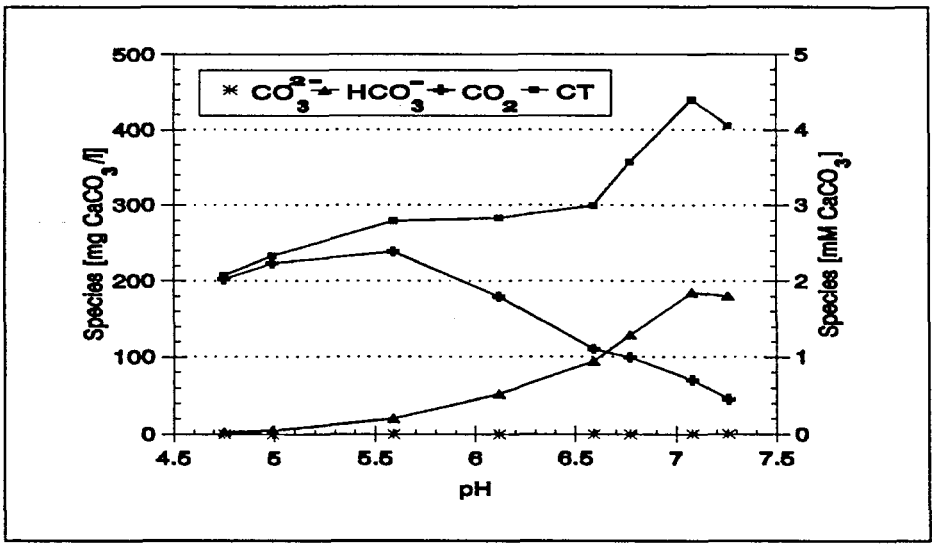

Fig. 4-9. The influence of pH on the carbonate species after cascade degassing

4.3.5 Crystallization

The results of three weeks continuous operation of the crystallizer are graphically depicted in Fig. 4-10. The pH values of the feed and effluent are displayed at the top, and the o-phosphate concentrations of the feed, filtered effluent, [Eff(F)], and acidified effluent, [Eff(A)], are displayed in the lower part of the figure. Fig. 4-11 represents the same data but with the effluent o-phosphate concentrations expressed as a percentage of the feed concentration.

The filtered effluent reflects only the o-phosphate remaining in solution, while the acidified effluent includes both the o-phosphate in solution and phosphate in flocs. The difference between the filtered and acidified effluents, Eff(A-F), thus represents the o-phosphate 'carried-over' as amorphous flocculated particles.

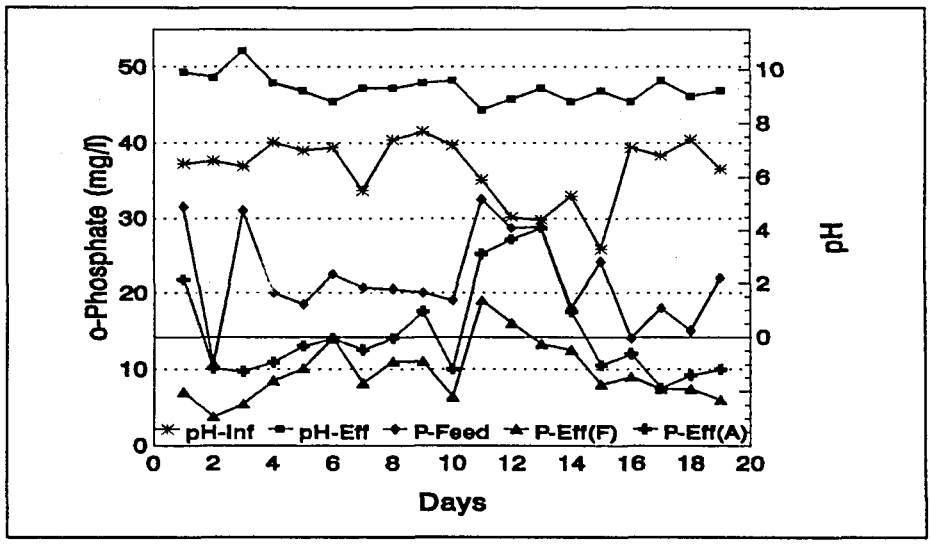

Fig. 4-10. Crystallizer influent and effluent pH and o-phosphate concentrations

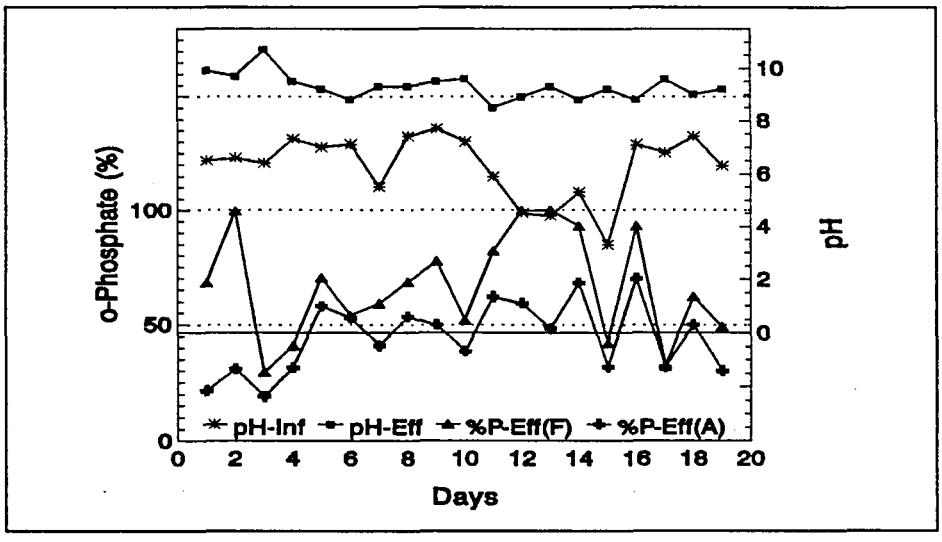

Fig. 4-11. Percentage of the crystallizer feed o-phosphate remaining in the effluent

Generally, for a specific feed pH, a high fraction of the effluent o-phosphate in the solid flocculated form would indicate a too high crystallization pH, while a high fraction of the feed o-phosphate still in solution in the effluent signifies a too low crystallization pH. This means that there is an optimum crystallization pH for the combination of lowest o-phosphate in solution and o-phosphate flocculated.

The most significant feature of Fig. 4-10 is probably the irregularity of all the graphs. The feed o-phosphate varied between a minimum of 10,3 mg P/ℓ and a maximum of 32,2 mg P/ℓ, with an average of 21,8 mg P/ℓ. The influent o-phosphate concentration is one of the prime driving forces in the crystallization reaction kinetics and thermodynamics. Thus the variation in concentration would influence both the rate and extent of the crystallization reaction.

Of greater concern is the variation in pH of the effluent (or crystallization), despite the fact that the PLC pH controller was set to maintain a constant pH of 9,60. Because pH relates to the logarithm of the hydroxide concentration, which also is a prime driving force in the crystallization reaction, it means that pH is certainly the single parameter with the greatest effect on the crystallization reaction. (The practical problems encountered with the pH controller are discussed at length in *Appendix 2, Pilot plant operation*).

The variation in the pH of the feed is related to the acid dosing for investigation of the influence of degassing on crystallization performance. It may be necessary to utilise the computer intelligence to monitor the pH of the influent before entry into the crystallizer to calculate the amount of lime or sodium hydroxide to be dosed to achieve the preset pH. As a control, a pH check could be introduced after exiting the column. Current instrumentation and control technologies have progressed to such an extent that this accurate pH control could be achieved under such adverse conditions as experienced in the crystallizer.

The highest o-phosphate removal (72 %) was achieved on day 3 when the effluent contained 28 % of the feed o-phosphate (17 % in solution and 11 % flocs) at a crystallization pH of 10,7 and a feed pH of 6,4. The crystallization pH values for the experimental period were, on average, too low, bearing in mind that there are other factors besides pH which also influence the removal, albeit to a lesser extent, e.g. feed o-phosphate and carbonate concentrations.

For the four days from day 7 to day 10 the feed o-phosphate was relatively constant (between 18,1 mg P/ℓ and 22,5 mg P/ℓ), and the crystallization pH also reasonably stable (increasing from 9,3 to 9,6). On day 7 the o-phosphate removal was 41% at a feed pH of 5,5, and on day 10 the removal was 47% at a feed pH of 9,6. In contrast, the removal for days 8 and 9 were 33% and 23% at respective feed pH of 7,4 and 7,7 implying that a lower crystallization pH is required for a lower feed pH.

In section *4.3.4 Pilot scale degassing*, the maximum feed pH for adequate CO_2 degassing was shown to be 4,75. On the pilot plant, acidification with 32 % hydrochloric acid, to achieve a reduction of carbonate by degassing, presented many practical problems, which was the principal reason for the variation in the feed pH (see *Appendix 2, Pilot plant operation*). Degassing was accomplished only on the three days from day 12 to day 15, day 14 excluded.

The worst results for the period, were obtained on days 12 and 13 with essentially no o-phosphate removal, although 42% and 54% were respectively removed on days 12 and 13 in the solid flocculated form. This peculiarity, with no crystallization yet half the o-phosphate in the form of flocs, implies that the pH of 4,5 and 4,4 of the degassing feed had the effect of producing flocculated particles in preference to crystallization, especially considering the low crystallization pH of 8,9 and 9,3. This hypothesis is, however, based on the assumption that the reaction came to completion in the presence of the crystallization seed material, implied by the intensity of the kinetics of the reaction under consideration.

An alternative explanation, indirectly suggested by the absence of crystallization in the presence of simultaneous occurrence of high percentages of o-phosphate in solution and flocculated, would be that moderate conditions allowed the reaction to come to completion only after the reactants have already flowed through the fluidized bed, in which case no crystallization but only flocs would be produced. In such a case an increase in the crystallization pH would increase the reaction rates to complete the reaction in the presence of the fluidized seed material and thus yield a certain measure of crystallization. In fact, the last hypothesis seems even more probable when the results of day 15 are considered: an even lower degassing feed pH of 3,3 produced an effluent containing 42% of the feed o-phosphate (i.e. 58% removal), with 10% in the solid flocculated form.

On day 17 the crystallization pH of 9,6 produced an effluent containing 32 % of the 22,9 mg P/ℓ feed o-phosphate (68% removal), in solution. The fact that no flocks were formed, suggests that a higher crystallization pH might have given a better removal.

Although the results have been discussed as separate individual instances, it was not without regard for the memory effect of the process; the history of the process continuously influences its current performance. The main reasons for this is firstly recycling of the effluent back to influent of the reactor, and secondly the fact that the formation of crystals catalyses further crystallization.

These findings corroborate those in the literature, e.g. the full-scale DHV Crystalactor® at Westerbork achieves an average of 23% of the 7,5 mg P/ℓ feed o-phosphate in the crystallizer effluent, of which 16% is amorphous flocculated particles (1,2 mg P/ℓ) that are removed by the dual-media pressure filters, and the 0,5 mg P/ℓ filtered effluent is then recycled to dilute the influent to the reactor to 4,0 mg P/ℓ (see Table 4.2).

4.4 CONCLUSION

Whereas the variance of the results precludes any general steady-state conclusions, it provides results for different combinations of parameters for comparison.

The observed variability of the feed o-phosphate concentration is a significant parameter affecting the performance of crystallization.

The inability of the PLC system to sustain the stringent pH control requirements for efficient crystallization performance was one of the principal reasons for the relatively low and inconsistent o-phosphate removal accomplished. The main cause for this appears to be the inhibiting effect caused by a crystalline deposition on the pH measuring electrode (see *Appendix 2, Pilot plant operation*).

Degassing seems to increase the rate of o-phosphate crystallization and does not explain the high 'carry-over' of o-phosphate flocs.

The results indicate that sufficient crystallization cannot be achieved without concurrent 'carry-over' of o-phosphate flocs. While recycling is needed to stabilize the process, the recycled flocs have an adverse effect on the crystallization performance. Consequently, filter separation of the 'carry-over' flocs from the effluent before recycling may be required to obtain an effluent with a low o-phosphate concentration.

V. GENERAL CONCLUSIONS

5.1 ACHIEVEMENT OF OBJECTIVES

Phosphate crystallization technology is a relatively recent development and several unforeseen obstacles developed in upscaling to the pilot plant. This necessitated changes to the original objectives set for the investigation. The Steering Committee decided to concentrate the research efforts on the pilot-scale crystallization and no full-scale evaluation was conducted. The study on the effect of integration of the crystallizer into an activated sludge system was therefore also omitted as it was considered that this objective was of lesser importance and the probability of having a major influence on the performance of the activated sludge system would be small.

Although the emphasis in this investigation was on the pilot-scale evaluation, desk top simulation and laboratory experimentation was resorted to in order to obtain indicators more quickly on the direction to follow at pilot-scale. The limitations of the laboratory system at low flow rates resulted in the accrual of limited data on some objectives, particularly those subsidiary to correct design and proper operation. However, the data and knowledge gained in solving the problems fundamental to process performance was sufficient to provide a crystallizer design and consider operational aspects for the successful implementation of the crystallizer technology, integrated with municipal treatment works. Since the crystallization technology is relatively new and not established in South Africa, the economic evaluation of the system was discussed (see section 5-5). It would be of value of value to evaluate and collate performance data at pilot and full scale to improve the crystallizer design.

5.2 CHEMICAL MODELLING AND FULL SCALE APPLICATION

The application of dynamic chemical modelling using the Joint Expert Speciation System (JESS) proved to be time saving and cost effective in acquiring an insight into the relevant reactions. The crystallization process is governed by relative rates of precipitation of the compounds present in the effluent. Hydroxyapatite is the most stable with less stable compounds forming at the same time.

It was shown that carbonate removal is important to reduce the interference of $CaCO_3$ precipitation and that the concentration should not exceed 2 mM.

The practical application of the Crystalactor® by DHV corroborated the full-scale implementation of the crystallization technology in South Africa. Technical complexities, however, need careful consideration.

5.3 LABORATORY EVALUATION

The recycle ratio is an important parameter for consideration in efficient crystallization. Increasing the recycle ratio resulted in an increased hydraulic retention time at fixed total flow. This resulted in a dilution of the influent o-phosphate concentration, with a concomitant positive influence on the crystallization effectivity. At low recycle ratios, floc 'carry-over' increased whereas at high recycle ratios $CaCO_3$ crystallization occurred preferentially, increasing the concentration of uncrystallized o-phosphate in the effluent discharge.

In the laboratory system, effective venting of influent at low pH reduced the carbonate concentration by release of carbon dioxide, so that phosphate was preferentially removed from the effluent at all pH values.

The concentration of o-phosphate in the outflow continued to decrease with increasing pH, as was expected with low carbonate concentrations. This effect was not as noticeable at high recycle ratios where the reactor configuration more closely resembled a completely mixed, rather than a plug flow system. Thus, degassing in itself should have a beneficial effect when the other important performance criteria are also fulfilled.

5.4 PILOT-SCALE STUDIES

It was difficult to maintain optimum process conditions adequately in the pilot plant and the fluctuation of the results precluded any general steady-state conclusions. However, it provided results of different combinations of interacting parameters for comparison of the overall conditions required for effective crystallization.

The marked variability of the o-phosphate concentration in the feed had a significant influence on the crystallization performance.

Rigorous pH control must be maintained for efficient crystallization and proper process performance. The main cause for the erratic pH control appeared to be the interference caused by a crystalline deposition on the pH measuring electrode (see *Appendix 2, Pilot plant operation*).

At pilot scale, degassing appeared to intensify the o-phosphate crystallization, but with a simultaneous increase in 'carry-over' of o-phosphate flocs.

Under the prevailing conditions, considerable 'carry-over' of o-phosphate flocs was observed and sufficient crystallization could not be achieved. While an effluent recycle was needed to stabilize the process, the recycled flocs had an adverse effect on the crystallization performance. This indicated the requirement for filtration of the flocs from the effluent discharge before being recycled to ensure an effluent with a low o-phosphate concentration. Further investigation will therefore be required to resolve this problem.

5.5 ECONOMICS OF CRYSTALLIZATION

The minimum carbonate level for effective phosphate removal was considered to be 2 mM. Therefore, if carbon dioxide removal was essential, the treatment costs, using sodium hydroxide, amounted to approximately R2,11/m^3. This could be reduced to approximately R1,02/m^3 in degassing is not essential. The cost of chemicals for degassing thus contributed substantially to the treatment costs. However, it should be stressed that only a portion of the total anaerobic effluent needs to be treated to reduce the load on the biological phosphate removal system. Thus, if only 10% of the total effluent flow needs to be treated in a crystallizer, the foregoing costs, expressed in terms of total effluent flow, reduced to 21 cents/m^3 and 10 cents/m^3 respectively.

At the prevailing rates, the cost of using lime is only 27% of that of sodium hydroxide. However, the lower solubility of calcium hydroxide would require an additional mixing tank to produce milk of lime, and the savings in using lime would be partially offset by this extra cost. When calcium hydroxide is used instead of sodium hydroxide the overall operating cost is reduced by 26%.

5.6 TECHNOLOGY IMPLEMENTATION

The feasibility of phosphate crystallization has been demonstrated and the major design criteria established in Appendix 1. The following is necessary for the successful implementation of the technology:

- Careful crystallizer design, particularly of the inlet system and fluidized bed distributor, which has been thoroughly examined in the present investigation.

- Suitable quartz sand should be used as crystallization seed material in the fluidized bed.

- At the beginning of commissioning an adequately fluidized bed should be established at a linear upflow velocity of between 40 m/h to 80 m/h.

- For a full-scale crystallizer a maximum recycling ratio of 1 is used by DHV in The Netherlands. However, in the present investigation a recycle ratio of up to 7 was shown to be advantageous. The selection of recycle ratio therefore needs further clarification.

- The crystallizer influent Ca:P mass ratio should be as close as possible to the 2:1 stoichiometric requirement.

- Water with a high alkalinity requires effective CO_2 degassing to reduce the total carbonate to below 2 mM, preventing the precipitation of $CaCO_3$ in preference to HAP. This will maximise the mechanical strength of the crystals and minimize 'carry-over' of o-phosphate flocs.

- Sodium hydroxide (1%) or milk of lime (2%) can be used for pH control between 9,8 and 10,5 for effective crystallization; and concentrated sulphuric

acid (98%) for achieving the required degassing pH of 4,8 to 5,0. Although the lower solubility of lime ($Ca(OH)_2$) implies extra mixing equipment, it could be advantageous when calcium supplementation is required.

- An appropriate automated control system for stringent crystallization pH control is an unconditional requirement for effective process performance, with special consideration of the interference of crystallization on the pH measuring electrode.

- To achieve stable operational conditions for a full-scale crystallizer, a slow steady start-up period of 3 to 4 weeks is recommended (Eggers *et al.*, 1991a,b)

- For a final crystallizer effluent with a very low o-phosphate concentration (< 1 mg P/ℓ) removal of 'carry-over' flocs by filtration may be required, especially when a significant portion of the effluent containing flocs is recycled back to the crystallizer inlet.

5.7 FUTURE RESEARCH

The data obtained in laboratory investigations indicated that an increase in the recycle ratio from minimum fluidization to approximately 7 had a beneficial effect on the crystallization effectivity. For technical reasons reliable data on crystallization of phosphate could not be obtained in this region of recycling. However, DHV in The Netherlands used a recycle ratio of approximately 1. Further work should therefore be done to establish the optimum recycle ratio more accurately.

At higher recycle ratios, influent and the recycle stream mixing could result in phosphate precipitation before the sand bed above certain pH levels. Further work is required to preempt such precipitation and optimise the crystallization efficiency.

Degassing has been shown to be beneficial. However, further testing should be carried out under steady state conditions.

Lack of data on the cost-effectivity of filtration, as an adjunct to the crystallization column, makes it imperative that this aspect be further investigated. The need for such investigation was also indicated by the fact that DHV in The Netherlands, who have implemented the crystallization technology at full scale in Europe, made use of filtration in the systems configuration used in their full scale plants.

Full-scale crystallization has not been possible in this investigation. To ensure proper design specifications, therefore, full-scale evaluation of phosphate crystallization should be conducted. Such studies will contribute to the establishment of the technology in South Africa.

Recovery of phosphate is considered to be a benefit of the technology. The best method of abstraction of large pellets and the frequency of such abstraction during operation needs clarification.

Eggers E, Dirkzwager A H & van der Honing H. 1991a. Full-scale experiences with phosphate crystallization in a Crystalactor®. *Wat. Sci. Tech.*, **23**, 819-824.

Eggers E, Dirkzwager A H & van der Honing H. 1991b. Full-scale experiences with phosphate crystallization in a Crystalactor®. *Wat. Sci. Tech.* **24**, 333-334.

Ferguson, J F & McCarty, P L. 1971. Effects of carbonate and magnesium on calcium phosphate precipitation. *Environ. Sci. Technol.*, **5**: 534-540.

Ferguson, J F, Jenkins, D & Eastman, J. 1973. Calcium phosphate precipitation at slightly alkaline pH values. *J. Water Pollut. Contr. Fed.*, **45**: 620-631.

Ferguson, J F, Jenkins, D & Stumm, W. 1970. Calcium phosphate precipitation in wastewater treatment. *Chem. Eng. Prog. Symp. Ser.*, **67**: 279-287.

Freche, M & Heughebaert, J C. 1989. Calcium phosphate precipitation in the 60-80 °C range. *J. Cryst. Growth*, **94**: 947-954.

Heughebaert, J C, de Rooij, J F & Nancollas, G H. 1986. The growth of dicalcium phosphate dihydrate on octacalcium phosphate at 25 °C. *J. Cryst. Growth*, **76**: 192-198.

Hirasawa, I & Toya, Y. 1990. Fluidized-bed process for phosphate removal by calcium phosphate crystallization. *Am. Chem. Soc. Symp. Ser.*, **438**: 355-363.

Inskeep, W P & Silvertooth, J C. 1988. Kinetics of hydroxyapatite precipitation at pH 7.4 to 8.4. *Geochim. Cosmochim. Acta*, **52**: 1883-1893.

Janssen, P M J, Rensink, J H & Eggers, E. 1991. A promising combination of two phosphate removal techniques: Biological P-removal and the Crystalactor. *Water Sci. Tech.*, **24**: 329-332.

Jenkins, D. Menar, A B & Ferguson, J F. 1972. Recent studies of calcium phosphate precipitation in waste waters. **In**: *Applications of new concepts of physico-chemical wastewater treatment.* Eckenfelder, W W & Cecil, L K (Eds), *Prog. Wat. Technol.*, **1**: 211-230.

Joko, I. 1984. Phosphorus removal from wastewater by the crystallization method. *Water Sci. Tech.*, **17**: 121-132.

Jorgenson, S E, Libor, O & Barkacs, K. 1973. Investigation of phosphorus removal from water. *Water Res.*, **7**: 1885-1897.

Kaneko, S & Nakajima, K. 1988. Phosphorus removal by crystallization using a granular activated magnesia clinker. *J. Water Pollut. Contr. Fed.*, **60**: 1239-1243.

Kokobori, K & Kyosai, S. 1982. Development of crystallization process for phosphorus removal. *Public Works Res. Inst. Tech. Memo. No. 1889*, Japan.

Koutsoukos, P, Amjad, Z, Tomson, M B & Nancollas, G H. 1980. Crystallization of calcium phosphates: A constant composition study. *J. Am. Chem. Soc.*, **102**: 1553-1557.

VI. REFERENCES

Abbona, F, Franchini-Angela, M & Boistelle, R. 1992. Crystallization of calcium and magnesium phosphates from solutions of medium and low concentrations. *Cryst. Res. Technol.*, **27**: 41-48.

Barone, J P & Nancollas, G H. 1978. The seeded growth of calcium phosphates. The kinetics of growth of dicalcium phosphate dihydrate on enamel, dentin and calculus. *J. Dent. Res.*, **57**: 153-161.

Benefield L D, Judkins J F & Weand B L. 1982. *Process Chemistry for Water and Wastewater Treatment.* Prentice Hall, New Jersey.

Bischoff, J L & Fyfe, W S. 1968. Catalysis, inhibition and the calcite-aragonite problem I. The aragonite-calcite transformation. *Am. J. Sci.*, **266**: 65-79.

Boistelle, R & Lopez-Valero, I. 1990. Growth units and nucleation: The case of calcium phosphates. *J. Cryst. Growth*, **102**: 609-617.

Boskey, A L & Posner, A S. 1976. Formation of hydroxyapatite at low supersaturation. *J. Phys. Chem.*, **80**: 40-45.

Brown, J L. 1980. Calcium phosphate precipitation in aqueous calcitic limestone suspensions. *J. Environ. Qual.*, **9**: 641-644.

Brown, W E. 1973. Solubilities of phosphates and other sparingly soluble compounds. **In**: *Environ. Phosphorus Handbook*, Griffith, E J (Ed), Wiley, New York, pp 203-239.

Brown, W E & Chow, L C. 1981. Thermodynamics of apatite crystal growth and dissolution. *J. Cryst. Growth*, **53**: 31-41.

Dalas, E & Koutsoukos, P G. 1989. The growth of calcium phosphate on ceramic surfaces. *J. Mater. Sci.*, **24**: 999-1004.

Deitz, V R, Rootare, H M & Carpenter, F G. 1964. The surface composition of hydroxylapatite derived from solution behavior of aqueous suspensions. *J. Colloid Sci.*, **19**: 87-101.

Department of Water Affairs. 1986. *Management of the water resources of the Republic of South Africa.* Government Printer. Pretoria.

De Rooij, J F, Heughebaert, J C & Nancollas, G H. 1984. A pH study of calcium phosphate seeded precipitation. *J. Colloid Interface Sci.*, **100**: 350-358.

Eggers E. & Kiestra H. 1988. *Der Kornreaktor zur Phosphatentfernung aus Abwasser: von Labor bis Grossmasstab*, ISSW-Seminar. Karlsruhe.

Eggers, E & Van Dijk, J C. 1986. Phosphorus removal by crystallization in a fluidized bed reactor. *Recycling in chemical water and wastewater treatment. Schriftenreihe ISWW Karlsruhe.*, **50**: 349-361.

Nancollas, G H & Wefel, J S. 1976. Seeded growth of calcium phosphates: Effect of different calcium phosphate seed material. *J. Dent. Res.*, **55**: 617-624.

Nancollas, G H, Amjad, Z & Koutsoukos, P. 1979. Calcium phosphates - Speciation, solubility and kinetic considerations. *Am. Chem. Soc. Symp. Ser.*, **93**: 475-497.

Nancollas, G H, Sawada, K & Schuttringer, E. 1983. Mineralization reactions involving calcium carbonates and phosphates. **In**: *4th Int. Symp. Biomineralization*, pp 155-169.

Nývlt, J. 1978. *Industrial crystallization, The present state of the art.* Verlag Chemie, Weinheim, 182 p.

Overman, A R, Chu, R L & McMahon, B R. 1983. A kinetic model of steady state phosphorus fixation in a batch reactor IV. Details of surface kinetics. *Water Res.*, **17**: 15-19.

Reddy, M M & Nancollas, G H. 1971. Crystallization of calcium carbonate I. Isotopic exchange and kinetics. *J. Colloid Interface Sci.*, **36**: 166-172.

Rootare, H M, Deitz, V R & Carpenter, F G. 1962. Solubility product phenomena in hydroxyapatite - water systems. *J. Colloid Sci.*, **17**: 179-206.

Smith, R W & Hwang, M-Y. 1978. Phosphate adsorption of magnesium silicates. *J. Water Pollut. Contr. Fed.*, **50**: 2189-2197.

Standard Methods. (1989) *Standard methods for the Examination of Water and Wastewater.* (Seventeenth ed.) APHA, AWWA & WPCF, New York.

Termine, J D & Posner, A S. 1970. Calcium phosphate formation in vitro I. Factors affecting initial phase separation. *Arch. Biochem. Biophys.*, **140**: 307-317.

Thomas, S A. 1991. Effects of some ions on the conversion of amorphous calcium phosphate to calcium hydroxyapatite in aqueous medium. *Bull.Chem. Soc. Ethiop.*, **5**: 11-20.

Tomažič, B & Nancollas, G H. 1975. The seeded growth of calcium phosphates. Surface characterization and the effect of seed material. *J. Colloid Interface Sci.*, **50**: 451-461.

Van Dijk, J C & Braakensiek, H. 1984. Phosphate removal by crystallization in a fluidized bed. *Water Sci. Tech.* **17:** 133-142.

Van Dijk, J C & Wilms, D A. 1991. Water treatment without waste material: Fundamentals and state-of-the-art of pellet reactors. Paper presented to the IWSA World Congress, Copenhagen, May 1991.

Van Kemenade, M J J M & de Bruyn, P L. 1987. A kinetic study of precipitation from supersaturated calcium phosphate solutions. *J. Colloid Interface Sci.*, **118**: 564-585.

Wade, P, Murray, K & Jooste, R. 1993. The chemistry of the Ca-Mg-PO_4-CO_3 system: A reference work. *Division of Water Technology, CSIR.*

Kunii D & Levenspiel O. 1969. *Fluidization Engineering.* John Wiley & Sons, New York.

LaMer, V K. 1962. Solubility behaviour of hydroxylapatite. *J. Phys. Chem.*, **66**: 973-978.

Levenspiel, O. 1972. *Chemical Reaction Engineering.* John Wiley & Sons Inc., New York, NY. pp. 253-314.

Marshall, R W & Nancollas, G H. 1969. Kinetics of crystal growth of dicalcium phosphate dihydrate. *J. Phys. Chem.*, **73**: 3838-3844.

Meyer, J L & Nancollas, G H. 1972. Effect of stannous and fluoride ions on the rate of crystal growth of hydroxyapatite. *J. Dent. Res.*, **73**: 1443-1450.

Momberg, G. 1993a. Phosphate crystallization in activated sludge systems. *Water Research Commission*, Report No 215/1/93.

Momberg, G. 1993b. Phosphate fixation in waste water by means of controlled struvite formation. *Water Research Commission*, Report No 250/1/93.

Momberg, G A & Oellermann, R A. 1992. The removal of phosphate by hydroxyapatite and struvite crystallization in South Africa. *Water Sci. Tech.*, **26**: 987-996.

Momberg, G A & Oellermann, R A. 1993. A comprehensive study on an iron-phosphate removal system. *Water Research Commission*, Report No 430/1/93.

Moutin, T, Gal, J Y, El Halouani, H, Picot, B & Bontoux, J. 1992. Decrease of phosphate concentration in a high rate pond by precipitation of calcium phosphate: Theoretical and experimental results. *Water Res.*, **26**: 1445-1450.

Myerson, A S. 1990. Crystallization research in the 1990's, an overview. *Am. Chem. Soc. Symp. Ser.*, **438**: 1-14.

Nancollas, G H. 1971. The nucleation and growth of calcium phosphate crystals. *Croat. Chem. Acta*, **43**: 261-266.

Nancollas, G H & Koutsoukos, P G. 1980. Calcium phosphate nucleation and growth in solution. *Prog. Cryst. Growth Charact.*, **3**: 77-102.

Nancollas, G H & Mohan, M S. 1970. The growth of hydroxyapatite crystals. *Archs. Oral Biol.*, **15**: 731-745.

Nancollas, G H & Tomažič, B. 1974. Growth of calcium phosphate on hydroxylapatite crystals. Effect of supersaturation and ionic medium. *J. Phys. Chem.*, **78**: 2218-2225.

Nancollas, G H & Tomažič, B. 1977. The kinetics of induced precipitation. *Croat. Chem. Acta.*, **50**: 83-92.

Nancollas, G H & Wefel, J S. 1972. Mechanism of crystal growth of calcium phosphates. *Pap. Natl Meet., Div. Water, Air Waste Chem., ACS*, **12**: 206-211.

Zhang, J, Ebrahimpour, A & Nancollas, G H. 1992. Dual constant composition studies of phase transformation of dicalcium phosphate dihydrate into octacalcium phosphate. *J. Colloid Interface Sci.*, **152**: 132-140.

Zoltek, J. Jr. 1974. Phosphorus removal by orthophosphate nucleation. *J. Water Poll. Contr. Fed.*, **46**: 2498-2520.

1.1.3 DHV Crystalactor® specifications

DHV developed the Crystalactor® from lab-scale, in 1978, to full-scale, in 1988, and through various publications on their experience indicated the basic design criteria summarised in Table 1.

1.2 Design calculations

It is generally known throughout fluidization technology that a critical factor determining the quality of fluidization is the design of the fluid distributor.

Phosphate crystallization requires additional demands of the inlet system as a prerequisite to good process performance, as revealed by Eggers & van Dijk (1986):

'... the mixing behaviour of flow in the entrance section of the reactor is extremely important to create optimum conditions for crystallization and to prevent the formation of amorphous flocs containing phosphate.'

Table 2 summarizes the most critical requirements of the inlet system, dictated by the fluidization requirements, together with the reaction kinetics and the nature of the crystals.

Table 2. Inlet distributor requirements

1.	Flow through the inlet distributor should be evenly spread out to ensure a stable well developed plug flow fluidized bed without channelling or slugging.
2.	Mixing of the alkali and water should be intensive, but at a rate avoiding localised high supersaturation which causes homogeneous nucleation.
3.	Mixing of the caustic soda and water should be in the presence of the fluidized grains that act as crystallization seed material.
4.	Turbulence at the inlet distribution and throughout the fluidized bed should be kept at a minimum to prevent abrasion of the mechanically fragile phosphate crystals.

1.2.1 Physical properties of the fluidized bed

1.2.1.1 Size distribution

The results of a sieve analysis of the sand used in the pilot plant crystalliser are listed in Table 3.

APPENDIX

1. PILOT PLANT DESIGN

1.1 Design criteria

The criteria for the design of a fluidized bed crystallizer revolve around the need to simultaneously satisfy the requirements of a properly fluidized bed and of optimum crystallization, which is qualitatively summed up below.

1.1.1 Fluidized bed

The fluid velocity and distribution must be sufficient to produce a fluidized bed wherein the sand particles are just far enough apart to present a maximum of free particles with surface area available for crystallization. This fluidized bed must also be stable with a minimum of turbulence to avoid scouring of the crystallized particles.

1.1.2 Crystallization

The reaction kinetics, characteristic of the specific reaction, prescribe the conditions (e.g. pH and concentration) for optimum crystallization. At these conditions crystallization takes place at a certain rate. The liquid flow rate carries these reacting chemicals at a certain velocity through the fluidized bed, which should be high enough to allow for sufficient crystallization before the water exits the fluidized bed.

Table 1. Basic Crystalactor® design criteria

DEGASSING PRETREATMENT	:	96 % H_2SO_4 at pH = 4.9 - 5.2
Required influent total carbonate (CT)		< 2 mM
SEED MATERIAL	:	filter sand
Seeding pellet diameter	:	0,3 - 0,6 mm
Crystal pellet diameter	:	1 - 2 mm
Fixed bed height (L_o)	:	2 m
REACTOR DIMENSIONS:		
Height	:	4 - 6 m
Diameter	:	1 - 4 m
FLOW RATES:		
Linear upflow velocity (u)	:	40 - 80 m/h
Recycle ratio (R)	:	0 - 1
CRYSTALLIZATION CHEMICALS	:	2 % $Ca(OH)_2$ (milk of lime) or 1 % NaOH
Crystallization pH	:	10.0 - 10.5

Compiled from: Eggers & Kiestra (1988); Eggers *et al.* (1991a); van Dijk & Wilms (1991).

These values made it possible to compute the specific surface area of the sand bed:

$$S_b = \frac{6}{\rho_s \cdot \psi_s} \sum_{i-1}^{i-n} \left(\frac{\Delta \phi_i}{Dp_i} \right) = 6{,}6948 \text{ m}^2/\text{kg}$$

The density and viscosity of the crystallizer influent were assumed to be of the same order as that of pure water:

$$\rho_m = 0{,}9982 \text{ g/cm}^3 \qquad \mu_m = 1{,}002 \times 10^{-3} \text{ N·s/m}^2$$

1.2.2 Minimum fluidizing velocity

The pilot plant was operated at a number of different flow rates to determine the relationship between the fluidized bed height and the linear fluid velocity through the column. The results of the investigation are illustrated in Fig. 1, which was used to interpolate the minimum velocity needed at the onset of fluidization:

$$u_m^\circ = 38{,}72 \text{ m/h} = 0{,}01076 \text{ m/s}$$

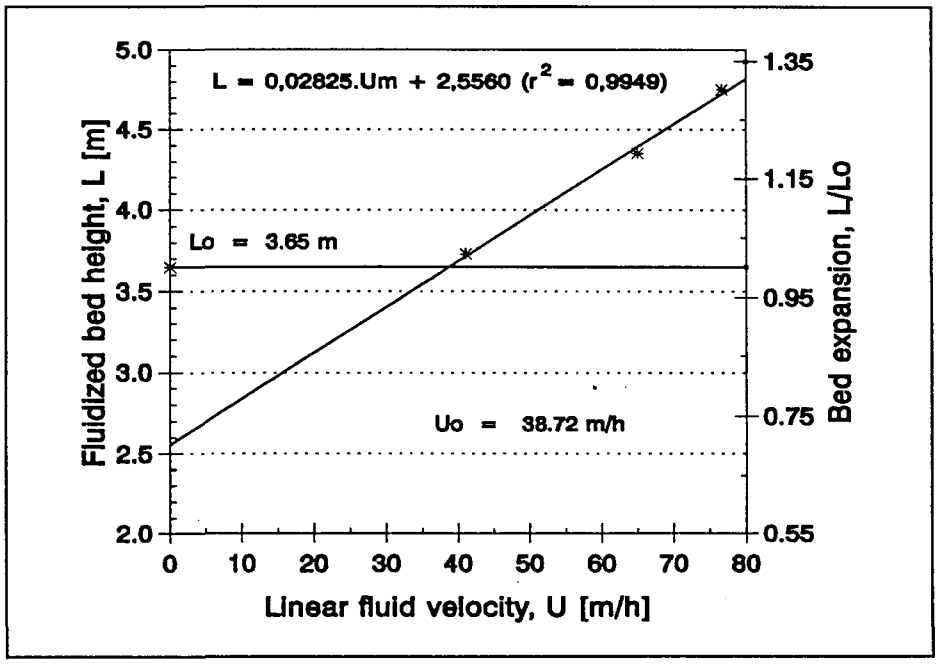

Fig. 1. Fluidized bed height as a function of the linear fluid velocity

1.2.3 Pressure drop through the fluidized bed

At low flow rates in a not yet fluidized bed the pressure drop is approximately proportional to the fluid velocity, reaching a maximum at the onset of fluidization. At the commencement of fluidization the packed bed suddenly 'unlocks', resulting in a

Table 3. Weight distribution of the sand particle sizes

Sieve size [mm]	Average diameter Dp [mm]	Cumulative mass fraction ϕ [w/w]	Mass fraction at Dp $\Delta\phi$ [w/w]
2,36		0,000	
	1,77		0,001
1,18		0,001	
	0,89		0,481
0,60		0,482	
	0,45		0,426
0,30		0,908	
	0,225		0,057
0,15		0,965	
	0,1125		0,023
0,075		0,988	
	0,05625		0,012
0,0375		1,000	

The weight-averaged particle diameter for the sand was calculated from the data in Table 3.

$$Dp = \sum_{i=1}^{i=n} (Dp_i \cdot \Delta\phi_i) = 0,6376 \text{ mm}$$

1.2.1.2 Density, voidage and sphericity

The solid density and bulk density of the sand were experimentally determined to be:

$\rho_s = 2,6485 \text{ g/cm}^3$ $\rho_b = 1,3772 \text{ g/cm}^3$

The fraction of voids (voidage) in the unfluidized sand bed was calculated from these densities:

$$\epsilon_b = \left(1 - \frac{\rho_b}{\rho_s}\right) = 0,4800$$

The voidage was in turn used to read off the sphericity of the sand from a graph by Brown *et al.* (1950), as presented by Kunii & Levenspiel (1969):

$$\psi_s = \left(\frac{\text{surface of sphere}}{\text{surface of particle}}\right)_{\substack{\text{same} \\ \text{volume}}} = 0,7305$$

The fraction of open area in the distributor plate was then determined as the ratio:

$$\frac{u_o}{u_{or}} = \frac{0{,}01076}{2{,}2602} = 0{,}004759$$

Lastly it was necessary to decide on a practical combination of orifice diameter and number of orifices. The values in Table 4 were calculated from the relationship:

$$N_{or} = \frac{u_m^o}{u_{or}} \frac{4}{\pi} \frac{1}{d_{or}^2} = \frac{0{,}006061}{d_{or}^2}$$

Table 4. Distributor orifice size and number combinations

Orifice diameter d_{or} [mm]	Specific number of orifices N_{or} [1/mm²]	Total number of orifices
1,0	0,006061	428
2,0	0,001515	107
3,0	0,0006735	48
3,5	0,0004948	35
4,0	0,0003788	27
4,5	0,0002993	21
5,0	0,0002425	17
5,5	0,0002004	14
6,0	0,0001684	12
8,0	0,0000947	7

An engineering drawing of the crystallizer inlet system is given in Fig. 2, and the details of the distributor plate illustrated in Fig. 3.

1.2.5 Nozzle sizing

Eggers & van Dijk (1986) demonstrated that optimum phosphate crystallization is accomplished with nozzles producing a minimum turbulence. In order to still ensure proper mixing of the sodium hydroxide and influent, under such conditions, it is thus necessary to strongly dilute the sodium hydroxide and inject it through nozzles with a relatively small orifice.

A simple neutralization titration of 1 ℓ influent showed that 4 mℓ of a 0,25 N NaOH solution (1 % NaOH) is required to raise the pH from 7,2 to 10,0.

slight decrease in the maximum pressure drop to the static pressure of the bed. With a further increase in the minimum fluidization velocity the pressure drop remains practically unchanged. This can be explained by the fact that the bed now acts as a fluid which deforms easily without appreciable resistance.

The pressure drop at the minimum fluidizing velocity was calculated from a correlation by Ergun (1952), as cited by Kunii & Levenspiel (1969):

$$\frac{\Delta P}{L} = 150\frac{(1-\epsilon_m)^2}{\epsilon_m^3}\frac{\mu_m \cdot u_m^o}{(\psi_s \cdot Dp)^2} + 1{,}75\frac{(1-\epsilon_m)}{\epsilon_m^3}\frac{\rho_m \cdot (u_m^o)^2}{\psi_s \cdot Dp}$$

$$\Delta P = 3{,}5[\ 18227 + 2045\ ] = 70953\ Pa$$

For liquid systems this pressure drop is further divided to indicate the contribution of the liquid weight:

$$\Delta P = \Delta P_b + [\epsilon_b \cdot \rho_m + (1-\epsilon_b) \cdot \rho_s] \cdot g \cdot L$$

$$= 7185\ Pa + 63768\ Pa$$

1.2.4 Distributor design

Experience shows that distributors should have a sufficient pressure drop to achieve equal flow through the openings. Kunii & Levenspiel (1969) recommend that the pressure drop across the distributor plate be roughly 10 % of the pressure drop across the bed, with a minimum of 3,5 kPa:

$$\Delta P_{d,min} = \max[\ 0{,}1 \cdot \Delta P_b\ ;\ 3{,}5\ kPa\ ] = 7{,}095\ kPa$$

The Reynolds number for the total flow approaching the distributor plate was used to select the corresponding value for the orifice coefficient C_d' from a graph by Perry (1963), adapted by Kunii & Levenspiel (1969):

$$Re = \left(\frac{D_b \cdot \rho_m \cdot u_m^o}{\mu_m}\right) = 3220 \qquad C_d' = 0{,}6$$

The velocity of the fluid through the orifices was calculated using this coefficient:

$$u_{or} = C_d'\left(\frac{2 \cdot \Delta P_d}{\rho_m}\right)^{1/2} = 2{,}2602\ m/s$$

2. PILOT PLANT OPERATION

2.1 Commissioning

The first step in commissioning was to operate the pilot plant with water but without any chemical dosing. Every time the crystallizer was loaded with new sand, continuous operation of about two days was required to wash out all the dust and small particles, at flow rates that produced sufficient fluidization without losing the sand.

Once the wash water became clear, the next step was to determine the relationship between the fluidization of the sand and the flow rates (see section *4.3.1 Fluidization and flow rate*), in order to calibrate the feed and recycle flow rates.

The next step, as part of the research project, was to do tracer studies to test the ideality of the flow and mixing of the inlet system and fluidized bed, at the established flow rates (see section *4.3.2 Non-ideal flow and mixing behaviour*).

Subsequently sodium hydroxide was injected very slowly by manual operation of the PLC pH control system. At the established flow rate of 3 m^3/h the crystallizer residence time was 10 minutes. To suppress the formation of 'carry-over' o-phosphate flocs the pH was raised slowly to give the system time to adapt to the recycled stream at the 10 minute lag time. Once the pH was stabilized at the level required for crystallization, the PLC pH control system was switched from manual to automatic control. Generally, it took at least 8 hours to establish stable automatic pH control.

The construction period for the full-scale DHV Crystalactor® at Westerbork was seven months, and the whole process of commissioning took no less than 30 days (Eggers & Kiestra, 1988).

2.2 Operational experience

The two most difficult problems experienced on the pilot plant scale were crystallization pH control and cascade degassing after acidification.

2.2.1 pH control

With the installation of a process control system, one of the main objectives is to measure and manipulate the variable as close as possible to the place where control is to be exercised. The rationale is that, the further apart the points of measurement and manipulation are from each other as well as from the point of control, the greater is the lag time between registering and response - and the more difficult and unstable the control becomes. A greater lag time between the change of the control variable and the measurement thereof, gives the process more time to drift away from the set point before the control system reacts to rectify the change. Naturally, the control system can never undo the past, although modern control systems can to a certain extent predict and anticipate the behaviour of a process, depending on its steadiness.

The flow rate of 1 % sodium hydroxide required at an influent velocity of 60 m/h would thus be:

$$Q_{noz} = 0{,}004\frac{\pi}{4}(D_b)^2 u_m = 0{,}01696 \text{ m}^3/\text{h}$$

The total injection area needed at an injection velocity of 3,5 m/s was calculated as:

$$A_{noz} = \frac{Q_{noz}}{u_{noz}} = 1{,}3464 \times 10^{-6} \text{ m}^2$$

Again this area was used to select a practical combination of nozzle orifice size and number of nozzles, as listed in Table 5.

$$n_{noz} = \frac{4 \cdot A_{noz}}{\pi \cdot d_{noz}^2} = \frac{1{,}7143 \times 10^{-6}}{d_{noz}^2}$$

Table 5. Injection nozzle size and number combinations

Orifice diameter d_{noz} [mm]	Total number of nozzles
0,10	172
0,20	43
0,25	27
0,30	19
0,35	14
0,40	11
0,45	9
0,50	7
0,55	6
0,60	5

Eggers & Kiestra (1988) illustrated the practical significance of nozzles with a photograph of the distributor plate of a 0,6 m diameter DHV crystallizer showing about 20 nozzles. For a 0,3 m diameter crystallizer 5 nozzles would give the same distribution.

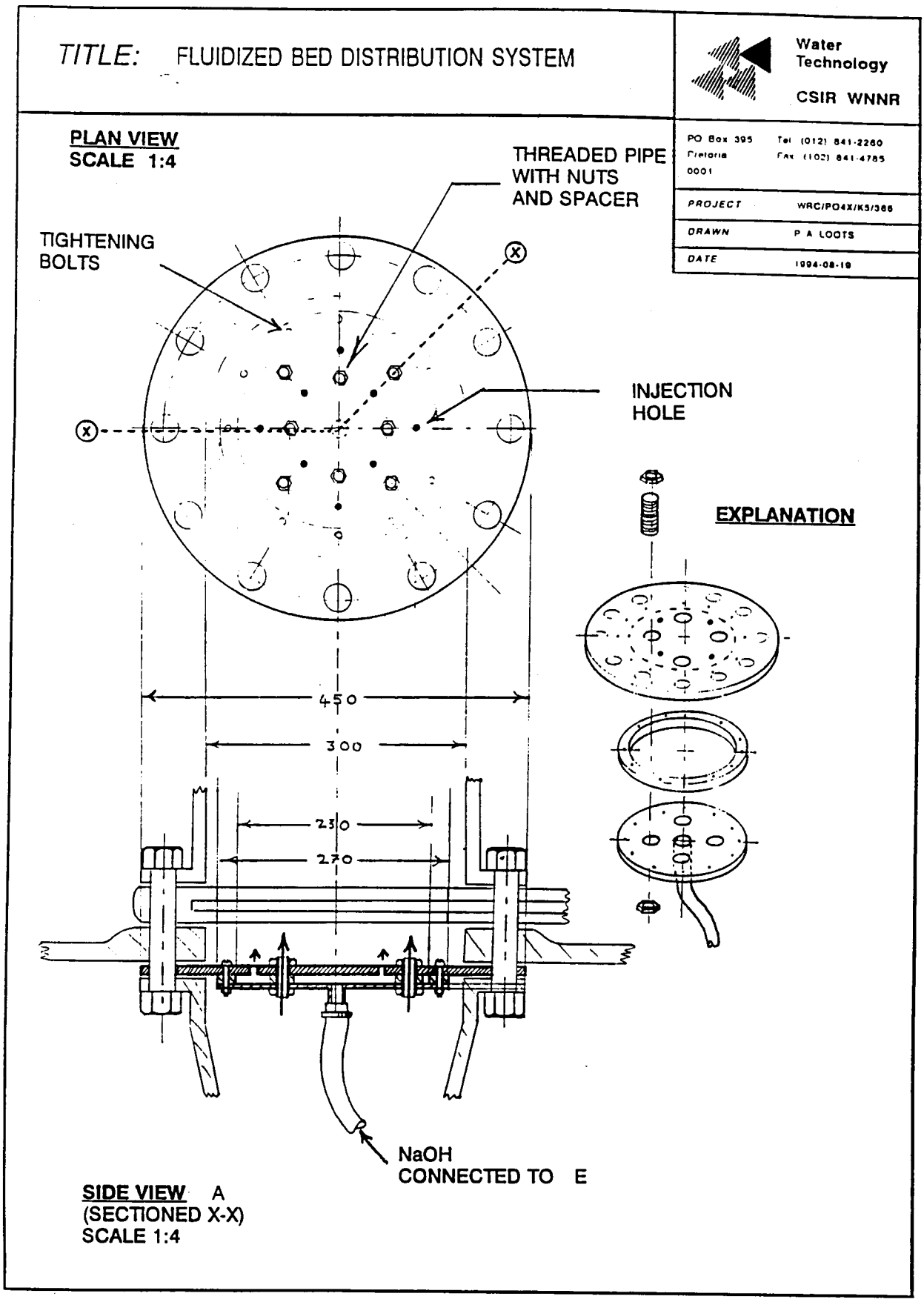

Fig. 3. Fluidized bed crystallizer distributor plate

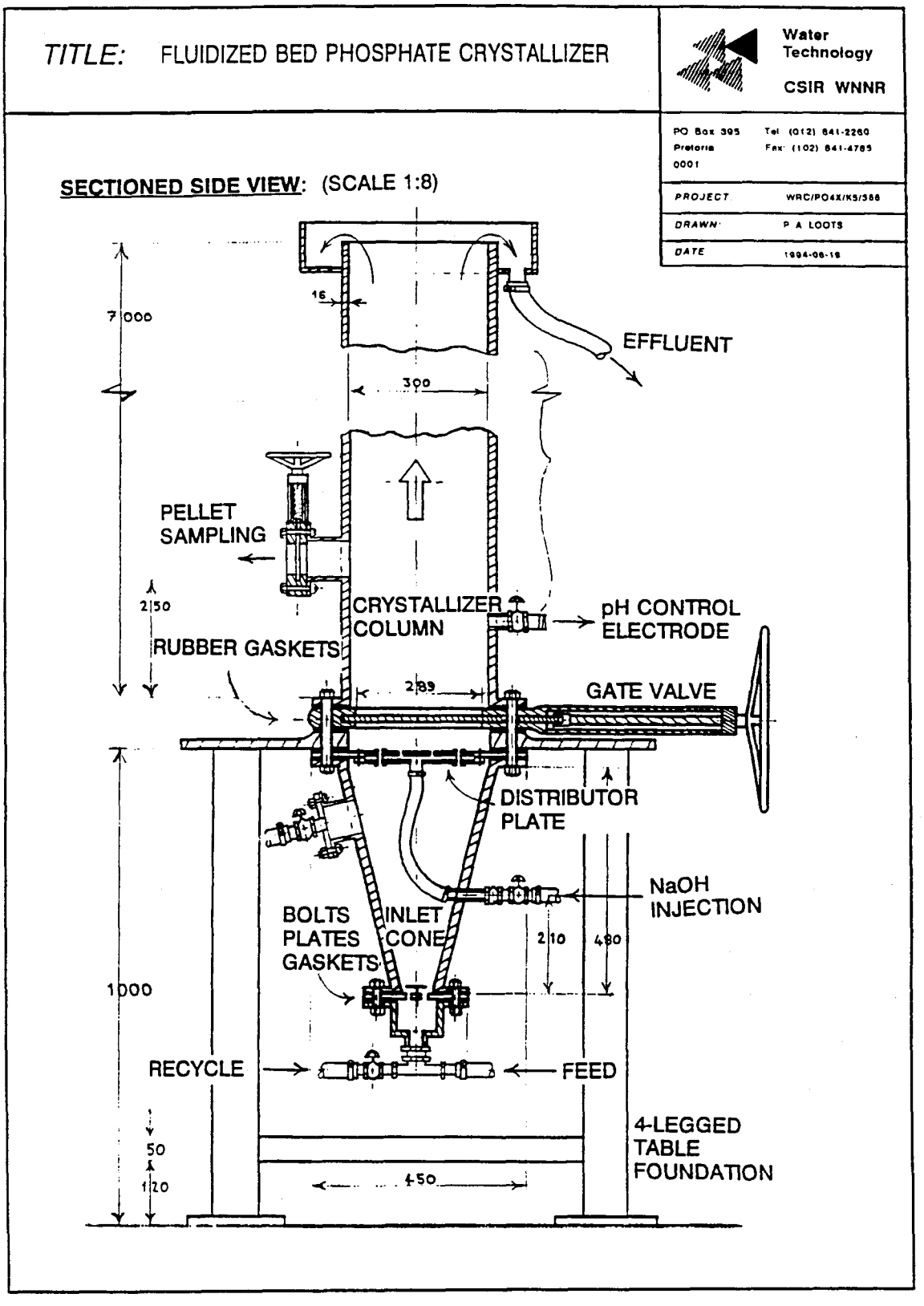

Fig. 2. Fluidized bed crystallizer inlet system

2.2.2 Degassing

The difficulties encountered with degassing were mainly due to the corrosive nature of the 32 % hydrochloric acid used for acidification (DHV uses 96 % sulphuric acid; Eggers *et al.*, 1991a). To decrease the supernatant pH to 4,75, required for degassing, an acid injection rate of ca. 17 mℓ/min was required. Numerous consultations with suppliers indicated that a peristaltic pump was the only way to achieve the required acid flow rate with variable control. The biggest acid resistant flexible tubing available was 2,5 mm ID, of which four pipes in parallel were unable to supply a sufficient flow rate of acid. To overcome this problem, the acid was gravitated from the crystallizer scaffolding tower, 3 metres above the supernatant outlet of the Settling Tank. This produced an adequate acid flow rate but with poor flow rate control.

3. COST EVALUATION

3.1 Operating cost

Table 6 lists the different components of the operating cost, with the respective quantities and cost rates involved when sodium hydroxide is used. Table 7 lists the same operating cost components but when calcium hydroxide is used.

Table 6. Estimated operating cost for the 43 m^3/d pilot plant phosphate crystallizer using sodium hydroxide

Operation cost component	Quantity	Rate	Cost [R/d]	Cost* [R/m^3]
CHEMICALS [kg/d; R/kg]				
1. NaOH (100 % Flakes)				
a. Un-acidified (no degassing)	4,61	2,32	10,70	0,0249
b. Neutralization (after degassing)	9,04	2,32	20,97	0,0488
2. Degassing with HCℓ (30 % m/m)	27,48	0,94	25,83	0,0601
ENERGY [kW.h/d; R/kW.h]				
Electricity	108	0,1	10,80	0,0251
WAGES [h/d; R/h]				
One operator ¾ h per day	0,75	30	22,50	0,0523
TOTAL COSTS			90,80	0,2112

* Based on 430 m^3/d main stream of which a 10% side stream is treated by the crystallizer

The pH in the pilot plant crystallizer was measured with a glass electrode, mounted in a 19 mm ID pipe connected to a sampling port situated 0,2 m above the distributor plate, where the sodium hydroxide was injected for crystallization pH control (Fig. 2).

Twice a day, sometimes three times a day, the electrode was dismounted, cleaned with a strong acid solution and thoroughly rinsed with clean water, before it was remounted. After cleaning the electrode glass appeared clear and shiny, but within about two hours of crystallization the electrode started to become clouded by a milky film. Furthermore, comparison with a calibrated portable pH meter revealed that, after cleaning, the pH registered by the controller was correct, but as the crystallization proceeded the controller pH deviated further from the correct value. This was also substantiated by the difference between the laboratory pH values of the samples and that indicated by the controller at the time of sampling.

A conceivable explanation is that the reacting chemicals crystallized on the glass electrode, in similar manner as that occurring on the sand of the fluidized bed, from where the water was taken for pH measurement. This film result in an interference with the measurement by the pH electrode, and consequently also with the control of the crystallization pH. Considering the importance of stringent crystallization pH control, this situation had unfortunate consequences on the crystallizer performance, as were revealed by the results.

The flow diagram of the DHV process indicates measurement of the crystallizer effluent, for crystallization pH control by sodium hydroxide injection at the inlet (Eggers & Kiestra, 1988). This implies a lag time of ca. 10 minutes between the points of measurement and manipulation, which presents a difficult process control situation that requires advanced control technology, depending on the stability of the process. However, the experience with the pH control of the pilot plant crystallizer probably explains why DHV, with their extensive experience in this field, employs this type of control system. The nature of this type of control system is possibly one of the reasons why it took 30 days to commission the full-scale Crystalactor® at Westerbork (Eggers & Kiestra, 1988).

It is evident that, for accurate pH control of the crystallizer, simultaneous monitoring of influent pH, amount of alkali required to achieve a preset pH, and effluent pH is essential. Current developments in process control systems allows simultaneous logical and computational capabilities in PLC's and loop controller-based systems to be placed directly on line and activate remote valves required for dosage. Such systems allow for consistency in monitoring and control of preset conditions to a high degree of accuracy. New pH sensors are available featuring control of contamination, clogging or coating ensuring prolonged performance at peak efficiency. Such systems may be considered for improved performance of the crystallizer.

Table 7. Estimated operating cost for the 43 m^3/d pilot plant phosphate crystallizer using calcium hydroxide

Operation cost component	Quantity	Rate	Cost [R/d]	Cost* [R/m^3]
CHEMICALS [kg/d; R/kg]				
1. $Ca(OH)_2$ (69 % Powder)				
a. Un-acidified (no degassing)	6,18	0,46	2,84	0,0066
b. Neutralization (after degassing)	12,12	0,46	5,58	0,0130
2. Degassing with HCℓ (30 % m/m)	27,48	0,94	25,83	0,0601
ENERGY [kW.h/d ;R/kW.h]				
Electricity	108	0,1	10,80	0,0251
WAGES [h/d; R/h]				
One operator ¾ h per day	0,75	30	22,50	0,0523
TOTAL COSTS			67,55	0,1571

* Based on 430 m^3/d main stream of which a 10% side stream is treated by the crystallizer

Comparison of Tables 6 and 7 show that, at the prevailing rates, sodium hydroxide is much more expensive to use than lime, the cost of which is only 27% of that for sodium hydroxide. However, the lower solubility of calcium hydroxide would require an additional mixing tank to produce milk of lime, and the cost savings in using lime would therefore be partially offset against this extra cost. When calcium hydroxide is used instead of sodium hydroxide the direct operating cost is reduced by 26% from 21 c/m^3 to 16 c/m^3 if degassing is required.

Another point to consider is the major impact of degassing on the operating cost. The reason for this is that the pH is first reduced to 4,8 to release carbon dioxide, and subsequently raised again to approximately 10,0 for the crystallization. This means that an additional amount of alkali, NaOH or $Ca(OH)_2$, is needed to neutralize the acid used for degassing. The cost of acidification and neutralization comprises as much as 52% of the operating cost when sodium hydroxide is used, and 46% when calcium hydroxide is used.

The cost structure appears favourable when the crystallizer is integrated into a biological phosphate removal plant to relieve the load on the system. Since the calculation is based on the treatment of a 10% sidestream, however, the actual treatment costs are an order of magnitude higher than those reflected. This must be taken into consideration for the treatment of effluent in other system configurations.